European Journal of Medicinal Chemistry 224 (2021) 113704

Contents lists available at ScienceDirect

European Journal of Medicinal Chemistry

journal homepage: http://www.elsevier.com/locate/ejmech

Discovery of *tert*-amine-based RORγt agonists

Ruomeng Qiu [a, 1], Mingcheng Yu [a, 1], Juwen Gong [a], Jinlong Tian [a], Yafei Huang [a], Yonghui Wang [a, *], Qiong Xie [a, b, **]

[a] Department of Medicinal Chemistry, School of Pharmacy, Fudan University, 826 Zhangheng Road, Shanghai, 201203, China
[b] Fudan Zhangjiang Institute, Shanghai, 201203, China

ARTICLE INFO

Article history:
Received 19 April 2021
Received in revised form
4 July 2021
Accepted 12 July 2021
Available online 14 July 2021

Keywords:
RORγt agonists
Tertiary amines
Th17 cell differentiation
Cancer immunotherapy
Small molecule drugs

ABSTRACT

The nuclear receptor retinoic acid receptor-related orphan receptor gamma-t (RORγt) is a transcription factor regulating Th17 cell differentiation and proliferation from naive $CD4^+$ T cells. Since Th17 cells have demonstrated the antitumor efficacy by eliciting remarkable activation of $CD8^+$ T cells, RORγt agonists could be applied as potential small molecule therapeutics for cancer immunotherapy. Based on the previously reported RORγt agonist **1** and its resolved co-crystal structure, a series of new tertiary amines were designed, synthesized and biologically evaluated, yielding optimal moieties with improved chemical properties and biological responses. The combination of these optimal moieties resulted in identification of novel RORγt agonists such as **8b** with further elevated RORγt agonism responses at a target-based level as well as in cell-based assays, which provided some structural knowledge for further optimization of RORγt agonists as small molecule therapeutics for cancer immunotherapy.

© 2021 Elsevier Masson SAS. All rights reserved.

1. Introduction

Cancer immunotherapy aims to exploit the immune system to attack tumors [1]. The immune suppression response of tumor can be altered by activating $CD8^+$ T cells through various mechanisms, including enzymes, receptors and cytokine signaling pathways [2–4]. T helper 17 (Th17) cells, a subset of $CD4^+$ T helper cells characterized by interleukin-17A (IL-17A) production, have been well-described in pathological processes of various human autoimmune diseases [5,6]. Recent study shows that Th17 cells and IL-17A expression have been found in a myriad of human tumors [7–11]. It has been demonstrated that Th17 cells have potential antitumor efficacy by triggering residential immunity responses to elicit remarkable activation of $CD8^+$ T cells [12].

The retinoic acid receptor-related orphan receptor gamma-t (RORγt) is a member of nuclear receptor (NR) superfamily, and it is the key transcription factor to drive naive $CD4^+$ T cells differentiated into Th17 cells [13,14]. Similar to other NR modulators, RORγt orthosteric ligands can display divergent mode of actions by inducing conformational change of the ligand binding domain (LBD) [14–21]. From the perspective of RORγt LBD promoting or reducing co-activator recruitment, the ligands can be classified as agonists, inverse agonists and neutral antagonists [22,23]. Since RORγt agonists have been shown to increase basal activity of RORγt and promote Th17 cell differentiation, development of RORγt agonists can be considered as a promising approach for cancer immunotherapy [24,25]. In clinical practice, cintirorgon (LYC-55716), a small molecule RORγt agonist developed by Lycera, has entered Phase 2 trial, supporting the feasibility of RORγt agonists being applied as orally bioavailable antitumor immunotherapeutic [26].

During structure-activity relationship (SAR) study of RORγt inverse agonists, GSK scientists serendipitously discovered a tertiary amine RORγt agonist **1** [17]. A co-crystal structure of RORγt LBD with agonist **1** was then resolved (PDB: 4NIE, resolution of 2.01 Å). The co-crystal structure revealed that the left-hand side (LHS) benzyl group of agonist **1** stabilized the hydrophobic site near Tyr502 of activation function 2 (AF2) domain (also known as H12), whose conformation was crucial for RORγt acting in an agonism manner by recruiting downstream co-activator peptide. Besides,

* Corresponding author.
** Corresponding author. Department of Medicinal Chemistry, School of Pharmacy, Fudan University, 826 Zhangheng Road, Shanghai, 201203, China.
E-mail addresses: yonghuiwang@fudan.edu.cn (Y. Wang), qxie@fudan.edu.cn (Q. Xie).

[1] R.Q. and M.Y. contributed equally to this work. R.Q., M.Y., Q.X., and Y.W. drafted the manuscript, conceived the experiments, oversaw the experimental design, and provided study supervision. R.Q., M.Y., J.G., J.T., and Y.H. carried out the synthesis and characterization of the compounds. M.Y. carried out the Th17 differentiation assay. All authors reviewed the manuscript.

https://doi.org/10.1016/j.ejmech.2021.113704
0223-5234/© 2021 Elsevier Masson SAS. All rights reserved.

adding 4-substituted bulky moieties at LHS phenyl ring of agonist **1** resulted in discovery of inverse agonists within the same chemical scaffold. The agonist **1** has good *in vitro* biochemical activity (EC_{50} = 7.8 nM,% maximum activation (% max act.) = 98.8% in our RORγt dual fluorescence resonance energy transfer (dual FRET) assay). However, agonist **1** was not able to promote mouse Th17 (mTh17) cell differentiation above basal activity, indicating that the molecular activity of agonist **1** was not sufficient to trigger cellular responses. Further study was expected to improve agonism of **1** and discover new RORγt agonists with good cell-based activity.

In this paper, based on the co-crystal structure of agonist **1** with RORγt LBD and mode of action, detailed SAR exploration and optimization of each region of agonist **1** has been carried out. A series of tertiary amines as RORγt agonists (Fig. 1) were designed, synthesized and biologically evaluated. By combining the dominant moieties of each region, the RORγt agonists such as **8b** with improved cell-based activities were identified as a potential lead compound for further optimization.

2. Results and discussion

2.1. Design and synthesis

In order to learn how the chemical modifications of each region on agonist **1** influence the binding mode and potential functionality, compounds with moieties of varying properties on LHS region, *N*-substituent (R_1), amino position (n, m), central phenyl ring (X, Y), linker and right-hand side (RHS) region were designed (Fig. 1) and synthesized following different synthetic procedures (Schemes 1–3).

2.2. Chemistry

The synthesis of *tert*-amine-based compounds **1**, **2a-2e**, **3a-3g**, **6b**, and **6c** is depicted in Scheme 1. The commercially available aldehydes (**9**) were first protected by ethylene glycol. Then the nitro-containing intermediates (**10**) were reduced to afford the corresponding anilines (**11**). Aldehyde intermediates (**13a**) were obtained through amide formation, followed by aldehyde deprotection reaction. Intermediates (**14**) were synthesized through reductive amination. The following alkylation with alkyl bromides yielded the target compounds. For compound **6c**, further reduction reaction was required using compound **1**. Specially, the preparation of compound **6b** started with a reversed amide (**13b**) formation reaction using 4-formylbenzoic acid (**12**) and (4-(ethylsulfonyl) phenyl)methanamine as substrates. Then it followed the remaining synthetic procedures depicted in Scheme 1.

The synthesis of compounds **2f-2h**, **4b-4g**, **5a-5c**, **6a, 7a-7e** and **8a-8c** is depicted in Scheme 2. The secondary amine intermediates (**16**) were obtained through reductive amination. Then a nucleophilic reaction with commercially available benzyls furnished the nitro intermediates (**18**). The reduction reaction followed by amide or urea formation afforded the target compounds.

Compounds **4a** and **4h-4k** were prepared via synthetic pathways shown in Scheme 3. Secondary amine intermediates (**20**) were obtained through nucleophilic reaction. A nucleophilic reaction and reduction reaction followed to afford amines (**22**). Then the target compounds were obtained through amide formation.

The synthesized compounds were then evaluated in RORγt dual FRET assay, Gal4 cell-based reporter gene assay, and mouse Th17 (mTh17) differentiation assay.

2.3. Modifications of LHS

The SAR of the LHS of agonist **1** was first explored (Table 1). The synthesized compounds were assessed at a target-based level by RORγt dual FRET assay, where the EC_{50} values signified potency and % max act. implied efficacy as complementary parameters of RORγt agonism. Substitution on the LHS phenyl ring (**2a-2e**) almost had no impact on the RORγt potency of the compounds, according to their EC_{50} values. However, for *ortho*-substituted compounds (**2a-2c**), the % max act. values decreased from 96.2% to 52.5% in the order of -F > $-CH_3$ > -Cl. Similarly, the -Cl substitution position on the LHS phenyl ring (**2c-2e**) notably decreased RORγt agonism response in

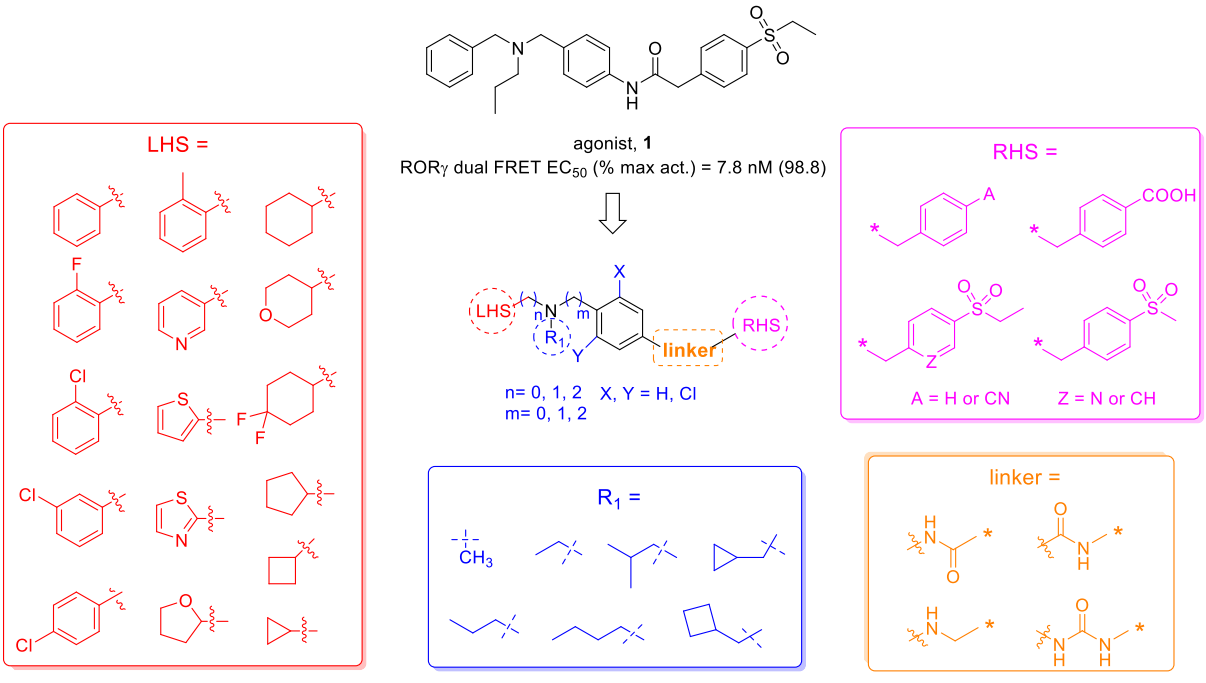

Fig. 1. Compound design for SAR exploration based on agonist **1**.

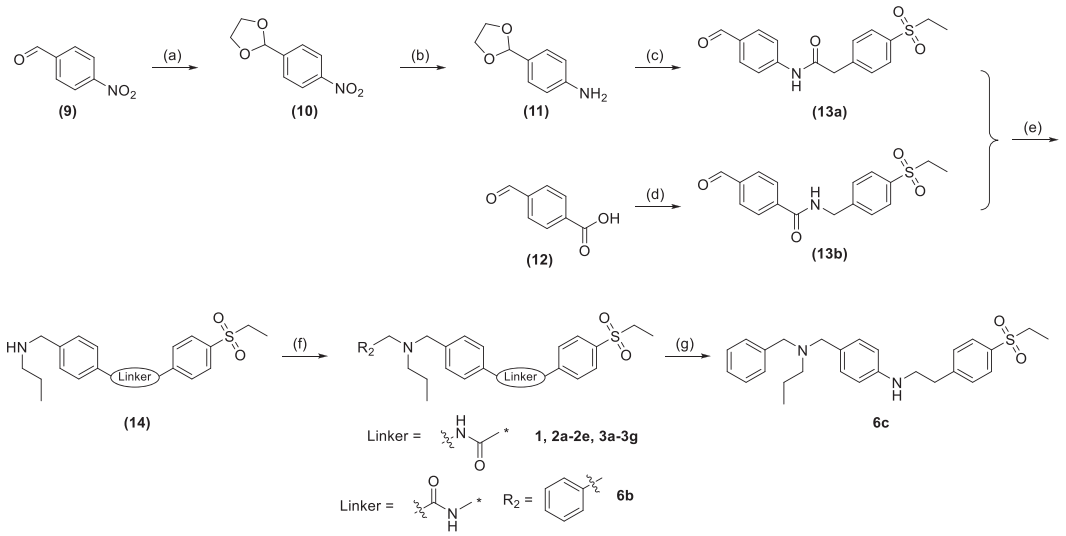

Scheme 1. General synthesis route 1[a].
[a] Reagents and conditions: (**a**) TsOH, glycol, and toluene under reflux (**b**) PtO_2, H_2, $NaHCO_3$ and MeOH at r.t. (**c**) DIPEA, HATU, 2-(4-(ethylsulfonyl)phenyl)acetic acid (**23**) and DCM at r.t. followed by 1 N HCl at r.t. (**d**) DIPEA, HATU, (4-(ethylsulfonyl)phenyl)methanamine and DCM at r.t. (**e**) *n*-propylamine, and DCM at r.t. followed by $NaBH_4$, and MeOH at r.t. (**f**) Bromine-substituted alkyl or aryl compounds, K_2CO_3 and DMF at 100 °C (**g**) BF_3·THF at 0 °C then r.t..

the order of *ortho* > *meta* > *para*. These results indicated that both size and position of the substituents on LHS would interfere with AF2 domain and thus reduce co-activator recruitment. Replacing phenyl ring with hetero-aryl ring (**2f**-**2h**) decreased both potency and efficacy, indicating the negative role of these heteroatom-containing moieties in RORγt agonism.

We then replaced LHS phenyl ring with a series of cycloalkyl moieties. With the increasing size of these moieties, the compounds exhibited improved potency and % max activation (**3a**-**3d**). Compound **3d** had a slightly decreased EC_{50} and higher maximum activation response (EC_{50} = 22.4 nM, % max act. = 106%) compared to agonist **1** (EC_{50} = 7.80 nM, % max act. = 98.8%), indicating certain size of LHS moiety is needed to stabilize AF2 domain that maintains RORγt agonism. However, when hetero-atoms substituted at LHS cycloalkyl ring (**3e**, **3f, 3g**), the activation level notably decreased, likely due to the increased hydrophilicity

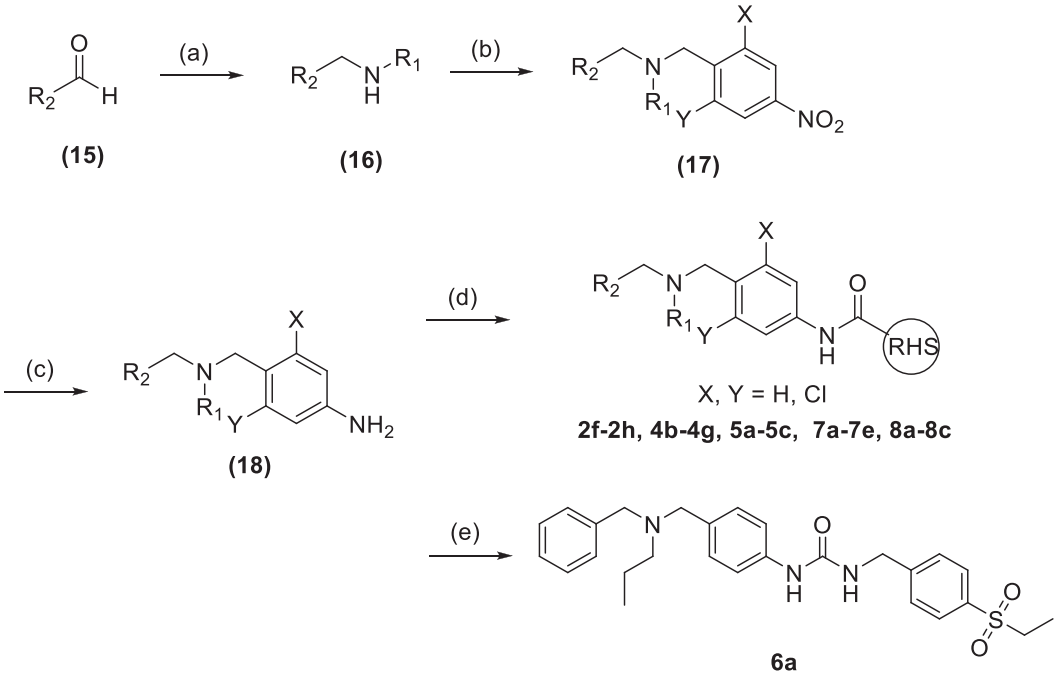

Scheme 2. General synthesis route 2[a].
[a] Reagents and conditions: (**a**) amines (R_1NH_2), and DCM at r.t. followed by $NaBH_4$, and MeOH at r.t. (**b**) substituted 4-nitrobenzyl bromides, K_2CO_3 and DMF at 100 °C (**c**) PtO_2, H_2, $NaHCO_3$ and MeOH at r.t. (**d**) DIPEA, HATU, 2-(4-(ethylsulfonyl)phenyl)acetic acid (**23**)/acids and DCM at r.t. (**e**) triphosgene, DIPEA, and THF at 0 °C, followed by (4-(ethylsulfonyl) phenyl)methanamine in THF at r.t..

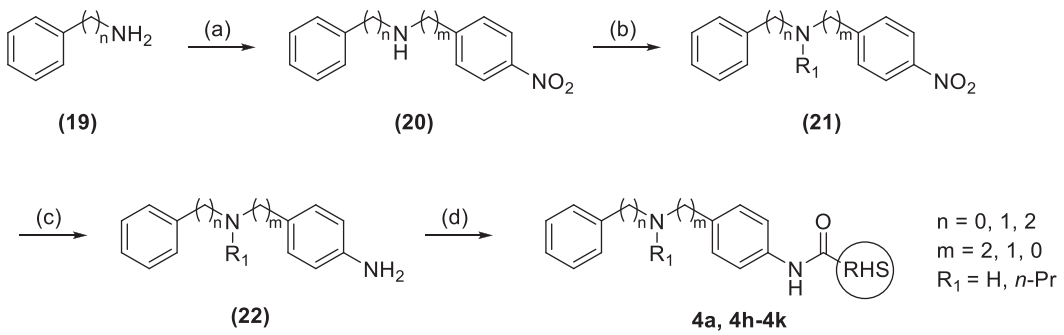

Scheme 3. General synthesis route 3[a].
Reagents and conditions: (**a**) Bromine-substituted benzenes or alkylbenzenes, K_2CO_3, KI, and MeCN at 110 °C, M.W. (**b**) 1-bromopropane, K_2CO_3, KI, and MeCN at 110 °C, M.W. (**c**) Pd/C, H_2, and MeOH at r.t. (**d**) DIPEA, HATU, 2-(4-(ethylsulfonyl)phenyl)acetic acid (**23**) and DCM at r.t..

Table 1
LHS SAR of the tertiary amine compounds.

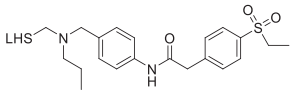

Cmpd.	LHS	RORγt dual FRET	
		EC_{50}[a] (nM)	% max act.[a]
1		7.80	98.8
2a		9.40	96.2
2b		11.6	70.5
2c		16.9	52.5
2d		18.7	42.1
2e		16.8	14.7
2f		29.1	63.4
2g		40.2	47.7
2h		>30000	N.D.[b]
3a		6530	16.9
3b		291	45.1
3c		109	101
3d		22.4	106
3e		79.6	14.0
3f		86.2	23.0
3g		285	80.5

[a] All results are an average of at least two runs of individual experiments.
[b] N.D.: no data.

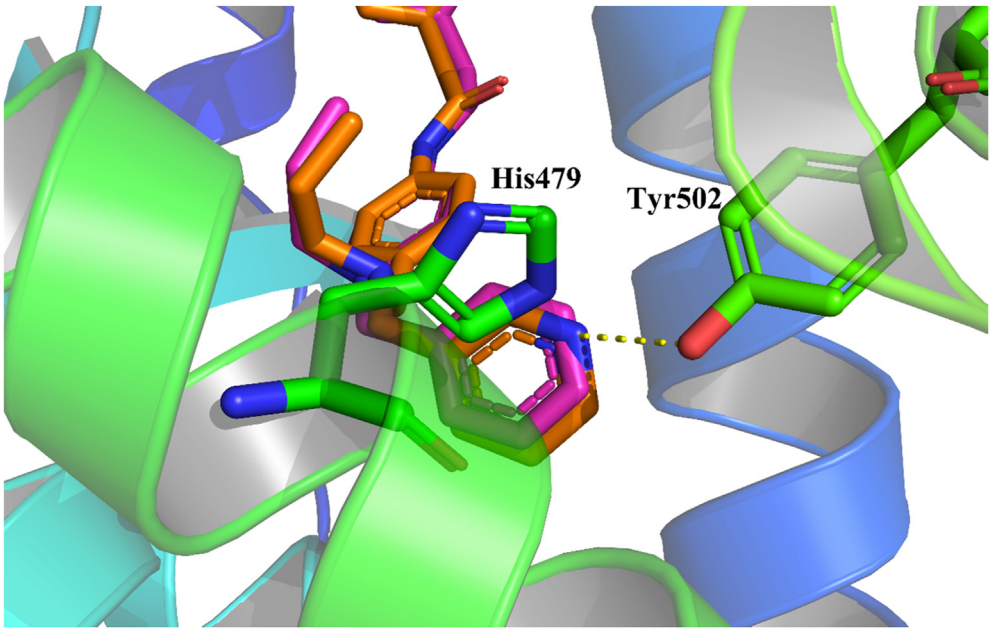

Fig. 2. Predicted binding mode of **2g** (in orange) overlay with co-crystal structure of **1** (in magenta) in RORγt LBD (PDB: 4NIE, resolution of 2.01 Å). Key residues of RORγt LBD, His479 and Tyr502, are displayed in green. Hydrogen bond was highlighted in yellow dash dot.

introduced by these moieties.

In order to explain the impact of LHS heteroatom alterations on biological function, we performed the molecular docking study using compound **2g**, which has the identical chemical structure with **1** except for pyridine moiety substitution on LHS. Despite of having a similar ligand conformation to **1** as shown by the overlay structure in RORγt LBD (Fig. 2), the nitrogen atom in pyridine moiety on LHS of **2g** formed hydrogen bonding with Tyr502, competing against the polar interactions between Tyr502 and His479. Previous studies have shown that Tyr502-His479 association in AF2 domain is critical to maintaining RORγt agonism [27]. We hypothesized that the presence of heteroatoms in LHS could disrupt the polar contacts of Tyr502 with His479, leading to destabilization of AF2 domain and decrease of RORγt agonism.

Table 2
SAR of *N*-alkyl of the tertiary amine

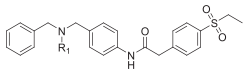

Cmpd.	R_1	RORγt dual FRET	
		EC_{50}[a] (nM)	% max act.[a]
4a	-H	>30000	N.D.[b]
4b	$-CH_3$	101	79.0
4c	$-CH_2CH_3$	36.3	85.1
1		7.80	98.8
4d		11.1	76.9
4e		10.8	66.5
4f		14.0	84.5
4g		7.10	82.0

[a] All results are an average of at least two runs of individual experiments.
[b] N.D.: no data.

2.4. Modifications of N-alkyl moieties

To explore the potential conformational effect of *N*-alkyl moieties on RORγt agonism, we then focused on the SAR study of *N*-alkyl of the tertiary amines (Table 2). Without *N*-alkyl substitution (**4a**), the potency dropped dramatically. Increasing size of *N*-alkyl moieties (**4b**, **4c**, **1**) improved both potency and % max activation in the order of Me < Et < *n*-Pr. However, further enlarged moieties (**4d**-**4g**) did not influence potency so much but lowered efficacy compared to agonist **1**.

Based on the structure of agonist **1**, the nitrogen atom was left-shifted or right-shifted (Table 3). For non-*N*-alkylated agonists (**4a**, **4h**, **4i**), right-shifted NH (**4h**) exhibited better RORγt agonism than the left-shifted NH (**4i**); besides, both **4h** and **4i** showed better activity than **4a**, which could be attributed to the adjusted

Table 3
SAR study of the *N*-shift of the tertiary amine.

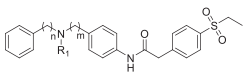

Cmpd	R_1	n	m	RORγt dual FRET	
				EC_{50}[a] (nM)	% max act.[a]
4a	-H	1	1	>30000	N.D.[b]
4h	-H	2	0	55.2	56.3
4i	-H	0	2	49.3	30.0
4j		2	0	11.6	85.7
4k		0	2	11.2	70.1
1		1	1	7.80	98.8

[a] All results are an average of at least two runs of individual experiments.
[b] N.D.: no data.

molecular conformation. For *N*-alkylated agonists (**1**, **4j**, **4k**), similar to non-*N*-alkylated agonists, right-shifted *N*-alkyl agonist (**4j**) displayed better RORγt agonism than the left-shifted (**4k**), but less than the compound **1**.

2.5. Modifications of middle phenyl ring

For the identified tertiary amine RORγt agonists (**1**, **4e**), a Cl group was introduced to the ortho-position of the middle phenyl ring (**5a**, **5b**, **5c**) (Table 4). Interestingly, the Cl group addition improved RORγt efficacy (**5a** vs. **1** ; **5b** vs. **4f**) while maintaining the potency; for the starting compound **1**, 2,6-diCl addition further improved the RORγt agonism, affording a potentially better RORγt agonist (**5c**). To obtain the structural insights of the enhanced agonism by introducing Cl group, we performed docking study of **5a** with co-crystal structure of RORγt LBD and **1** (PDB: 4NIE). As shown in the overlay structure (Fig. 3), the predicted molecular conformation of **5a** was mostly overlapped with **1**, which ensured hydrogen bonding formation with the key residues in RORγt LBD. Aside from the intramolecular interactions shown with agonist **1**, the Cl group of **5a** formed a halogen bonding with Cys320 (highlighted in yellow) of H3 in adjacent to AF2 domain (H12) in the RORγt LBD ternary structure. We speculate that the additional halogen bonding of **5a** with Cys320 stabilized AF2 domain as a preferred conformation for downstream co-activator recruitment, leading to enhanced efficacy. This explanation is also in accord with the further increase in potency of **5c**, as the 2,6-diCl substitution may endow a better chance to the compound forming halogen bonding with Cys320.

Table 4
SAR study of the central phenyl ring.

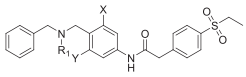

Cmpd	R_1	X	Y	RORγt dual FRET	
				EC_{50}[a] (nM)	% max act.[a]
1		-H	-H	7.80	98.8
5a		-Cl	-H	8.70	120
5b		-Cl	-H	8.00	101
5c		-Cl	-Cl	8.20	117

[a] All results are an average of at least two runs of individual experiments.

2.6. Modifications of linker

We next replaced the amide linker with urea, reversed amide and ethylamine (Table 5). The compound with urea linker (**6a**) achieved better RORγt agonism than **1** although the potency was slightly lowered. The reverse amide (**6b**) showed decreased RORγt maximum activation although the potency was mostly maintained compared to **1**, indicating that the subtle position shift of NH as the hydrogen bonding donor may affect the stabilization of hydrophobic pocket recruiting downstream co-activators that would determine the potential RORγt agonism. When the amide linker was replaced by ethylamine (**6c**), the compound became an RORγt inverse agonist instead of RORγt agonist, indicating that a flexible linker would disrupt the preferred molecular conformation for an RORγt agonist.

2.7. Modifications of RHS

The SAR of RHS substituents of the tertiary amine compounds was investigated (Table 6). Replacing ethyl sulfone with methyl sulfone (**7a**) decreased the potency, but the RORγt agonism response increased slightly. Also, considering **7a** has slightly lowered molecular weight and CLogP value compared to **1**, methyl sulfonyl group is more preferable for further optimization. Introducing the carboxylic group (**7b**) in place of ethyl sulfonyl group lowered the activity dramatically. And smaller substituents like -CN (**7c**) and -H (**7d**) decreased the activity, likely owing to these substituents not able to establish intermolecular forces with the RORγt ligand binding pocket. We also switched the benzene ring of RHS

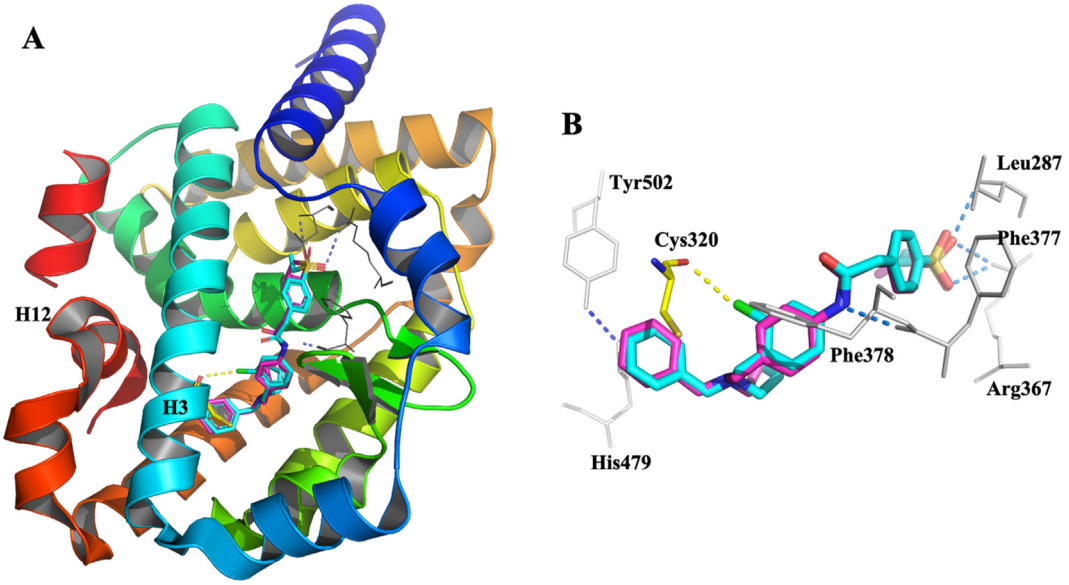

Fig. 3. (A) Predicted binding mode of **5a** (in cyan) overlay with co-crystal structure of **1** (in magenta) in RORγt LBD (PDB: 4NIE, resolution of 2.01 Å). (B) The key intramolecular interactions are shown in dash line. A halogen bond with Cys320 is highlighted in yellow.

Table 5
SAR of the amide linker replacement.

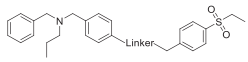

Cmpd	Linker	RORγt dual FRET	
		EC_{50}[a] (nM)	% max act.[a]
1		7.80	98.8
6a		58.0	118
6b		9.20	84.3
6c		33.6	−51.7

[a] All results are an average of at least two runs of individual experiments.

Table 6
SAR of RHS substituents of the tertiary amine.

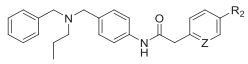

Cmpd	R_2	Z	MW	CLogP	RORγt dual FRET	
					EC_{50}[a] (nM)	% max act.[a]
1		-CH	464.62	4.25	7.80	98.8
7a		-CH	450.60	3.72	43.1	102
7b		-CH	416.52	5.10	>30000	N.D.[b]
7c		-CH	397.52	4.79	346	83.2
7d		-CH	372.22	5.36	2170	46.2
7e		-N	465.62	3.37	7100	N.D.[b]

[a] All results are an average of at least two runs of individual experiments.
[b] N.D.: no data.

into pyridine (**7e**) as an alternative approach to improving the hydrophilicity. Although **7e** had a lower CLogP value comparable to **7a**, it did not show significant potency and agonism on RORγt.

2.8. Combination of dominant moieties

According to the SAR investigation of LHS region, *N*-substituents as well as modifications on the central phenyl ring, linker and RHS region, we found that substituting the LHS with cyclohexyl moiety, adding Cl atoms to the central phenyl ring or replacing by methyl sulfone on RHS could all lead to the compounds with improved RORγt agonism. We thus hypothesized that the combination of these optimized moieties may result in the identification of compounds with greater potency and efficacy in the further bioactivity evaluation (Table 7). On the RORγt dual FRET assay, **8a**-**8c** achieved higher % maximum activation compared to **1**, which also exhibited high potency at nanomolar level. The *in vitro* activities of compound **1** and **8a-8c** were then evaluated in cell-based RORγt Gal4 reporter gene assay. Signified by activation maximum percentage on RORγt Gal4 assay, the RORγt agonism efficacy of **8a**-**8c** enhanced from 59.2% to 79.7% compared to agonist **1** (50.1%). We chose compound **8b** as a promising agonist for its overall potency and efficacy. A mouse Th17 (mTh17) cell differentiation assay that could better reflect the functionality was then performed to evaluate its bioactivity in promoting IL-17 production. We measured the proportion of IL-17 produced by mTh17 cells in flow cytometry and determined the percentage of activation relative to the vehicle with DMSO. In contrast with compound **1** that had no activity in promoting Th17 differentiation, compound **8b** promoted the production of IL-17 with a favorable EC_{50} value of 37.2 nM and a promising activation of around 30% above basal level (Fig. 4). By comparing the chemical structures of **8b** with **1**, we suspect that the cyclohexyl substitution on LHS has a more flexible molecular conformation that may increase the efficacy of being internalized by mTh17 cells, in contrast to rigid conformation caused by π-π stacking between the phenyl group on the LHS of agonist **1**.

To describe the drug-like properties of the lead compound, we assessed the kinetic solubility, predicted cell permeability and *in vitro* metabolic stability of **8b** in comparison with **1** (supplementary Table S1). Although the solubility of **8b** was not improved, compound **8b** showed enhanced predicted cell permeability and improved metabolic stability in mouse liver microsome. Enhanced cell permeability may partially contribute to the activity improvement in mTh17 assay. Yet, more efforts are needed for further optimization of the tertiary amine lead series.

3. Conclusions

Based on previously discovered tertiary amine agonist **1** and its resolved RORγt co-crystal structure, a series of tertiary amines were designed, synthesized and biologically identified as novel potent RORγt agonists. Consistently with our previous findings, LHS of tertiary amines was sensitive and crucial for RORγt agonism. Aside from LHS, SARs of other regions were also explored separately and led to the discovery of compounds (**3d**, **5a**, **5c**, **7a**) with better RORγt agonism or drug-like properties. The combination of these optimal moieties resulted in novel RORγt agonists (**8a-8c**) with further elevated RORγt agonism at target-based level as well as in cell-based assay, among which **8b** is superior in the mTh17 cell differentiation assay. This work provided some structural knowledge for further optimization of RORγt agonists as small molecule therapeutics for cancer immunotherapy.

4. Experimental

4.1. Materials and methods

All commercially available reagents and solvents were purchased and used without further purification unless otherwise stated. All reactions were monitored by TLC, using silica gel plates with UV light visualization. Column chromatography was performed using silica gel (200−300 mesh). ^{1}H NMR data was recorded on a Bruker 400 MHz NMR system. Chemical shifts in ^{1}H NMR spectra are reported in parts per million (ppm) on the δ scale relative to an internal control (TMS). Data are reported as follows: chemical shift (δ ppm), multiplicity (s = singlet, d = doublet, t = triplet, q = quartet, m = multiplet, dd = doublet of doublets, dt = doublet of triplets, br = broad), coupling constant in hertz (Hz), and integration. LC-MS data was recorded on Agilent Technologies 6120 quadrupole mass spectrometer. High-resolution mass spectra (HRMS) were obtained on an AB SCIEX TripleTOF 5600+ mass

Table 7
Activities of the compounds with combined chemical moieties.

Cmpd	Structure	RORγt dual FRET EC_{50} (nM)(% max act.)[a]	RORγt Gal4 EC_{50} (nM)(% max act.)[a]
1	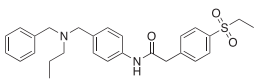	7.80 (98.8)	110 (50.1)
8a	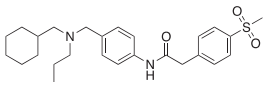	13.9 (108)	277 (59.2)
8b	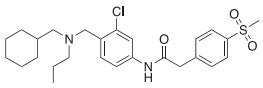	10.5 (111)	283 (72.1)
8c	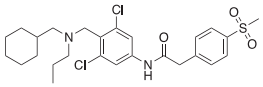	33.5 (115)	382 (79.7)

[a] All results are an average of at least two runs of individual experiments.

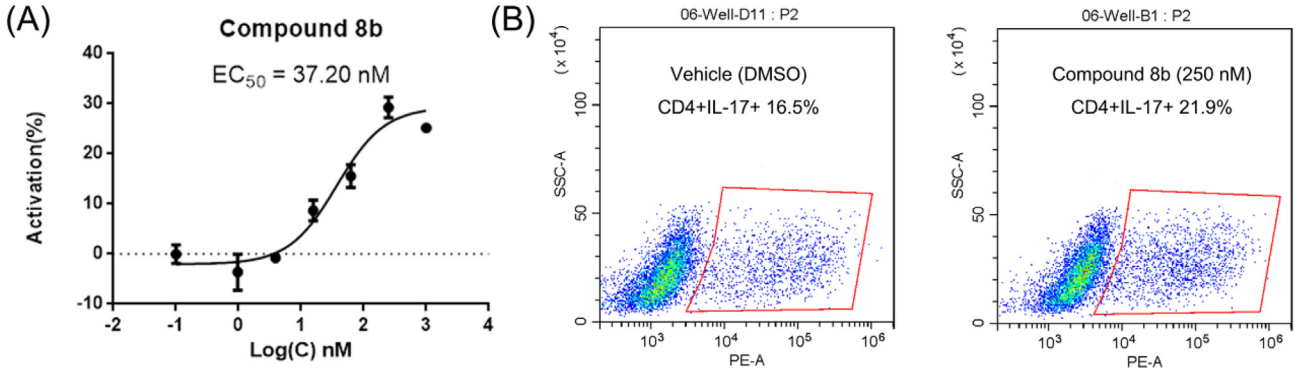

Fig. 4. RORγt agonist **8b** enhanced mTh17 cell differentiation and IL-17 production. (A) Dose-response curve obtained from stimulation of Th17 cells by **8b** at different concentrations. (B) **8b** increased the percentage of $CD4^{+}IL\text{-}17^{+}$ (Th17) cells at a concentration of 250 nM.

spectrometer (AB SCIEX, LLC., Redwood City, CA, USA). The contents of compounds for biological evaluation were examined with an Agilent 1260 Infinity LC system (Agilent Technologies, Inc., Santa Clara, CA, USA) with methanol/water (40:60 to 95:5) as the eluent. Unless specified, the purity of target compounds was >95%, which was considered to be pure enough for biological assays. The synthetic procedures, ^{1}H NMR, ^{13}C NMR and HRMS are detailed in the Supporting Information section.

4.2. Chemical synthesis

4.2.1. General procedure A for the synthesis of compounds (1, 2a-2e, 3a-3g, 6b)

Step 1. To a solution of 4-nitrobenzaldehyde (1.0 eq) and *p*-toluenesulfonic acid monohydrate (0.02 eq) in dry toluene was added ethylene glycol (3.0 eq). The mixture was heated up to reflux for 4 h. After cooling down, the solvent was removed under reduced pressure. The residue was purified by column chromatography on silica gel to afford the intermediate **10**.

Step 2. To a solution of 2-(4-nitrophenyl)-1,3-dioxolane (1.0 eq) and anhydrous sodium bicarbonate (1.0 eq) in methanol was added Adams' catalyst. The mixture was degassed and purged with hydrogen and stirred at room temperature for 4 h. The solution was filtered through celite and evaporated under reduced pressure to afford desired intermediate **11**.

Step 3. To a solution of 4-(1,3-dioxolan-2-yl)aniline (1.0 eq), 2-(4-(ethylsulfonyl)phenyl)acetic acid (1.2 eq) and HATU (1.2 eq) in DCM was gradually added DIPEA (3.0 eq). The mixture was stirred at room temperature for 4 h and was then added 1 N aqueous HCl, continuing to react for 1 h. The solution was basified by *sat.* Na_2CO_3, washed with brine, dried over Na_2SO_4 and evaporated under reduced pressure. Purification by column chromatography through silica gel afforded desired intermediate **13a.** The synthesis of **13b** followed the procedure of **13a.**

Step 4. To a solution of intermediate **13a** or **13b** (1.0 eq) and *n*-propylamine (2.4 eq) in dry DCM was added anhydrous Na_2SO_4 and stirred at room temperature overnight under nitrogen atmosphere. The mixture was filtered and evaporated under reduced pressure. The residue re-dissolved in methanol and was added $NaBH_4$ (0.5 eq), stirring at room temperature for 3 h. The reaction was quenched by saturated Na_2CO_3 and extracted with EA. The combined organic phase was evaporated to afford intermediate **14**.

Step 5. The mixture of **14** (1.0 eq), substituted benzyl bromide (3.0 eq) and anhydrous potassium carbonate (3.0 eq) in DMF was sealed and heated up to 60 °C for 3 h. The solution was washed with brine three times and the combined organic phase was evaporated.

Purification by column chromatography through silica gel afforded the target compounds (**1, 2a-2e, 3a-3g, 6b**)

*4.2.1.1. N-(4-((benzyl(propyl)amino)methyl)phenyl)-2-(4-(ethylsulfonyl)phenyl)acetamide (**1**).* Yield: 52%, white solid. ^{1}H NMR (400 MHz, DMSO) δ 10.25 (s, 1H), 7.86 (d, J = 8.0 Hz, 2H), 7.62 (d, J = 8.0 Hz, 2H), 7.56 (d, J = 8.2 Hz, 2H), 7.36–7.20 (m, 7H), 3.80 (s, 2H), 3.48 (d, J = 14.8 Hz, 4H), 3.28 (q, J = 7.3 Hz, 2H), 2.29 (t, J = 7.1 Hz, 2H), 1.52–1.40 (m, 2H), 1.10 (t, J = 7.3 Hz, 3H), 0.78 (t, J = 7.3 Hz, 3H). MS (ESI) m/z: 465.2 [MH+]. ^{13}C NMR (101 MHz, DMSO) δ 168.48, 142.69, 140.15, 138.18, 137.26, 134.98, 130.64, 129.33, 128.90, 128.60, 128.30, 127.18, 119.47, 57.96, 57.57, 55.13, 49.71, 43.42, 20.00, 12.20, 7.62. HRMS (m/z): [MH+] calcd for $C_{27}H_{33}N_2O_3S$ 465.2206; found, 465.2210.

*4.2.1.2. 2-(4-(ethylsulfonyl)phenyl)-N-(4-(((2-fluorobenzyl)(propyl)amino)methyl)phenyl)acetamide **(2a)**.* Yield: 59%, white solid. ^{1}H NMR (400 MHz, $CDCl_3$) δ 7.83 (d, J = 8.1 Hz, 2H), 7.66 (s, 1H), 7.51 (d, J = 8.1 Hz, 2H), 7.48–7.43 (m, 1H), 7.43 (d, J = 8.3 Hz, 2H), 7.29 (d, J = 8.2 Hz, 2H), 7.19 (dd, J = 12.9, 6.2 Hz, 1H), 7.08 (t, J = 7.2 Hz, 1H), 6.98 (t, J = 9.1 Hz, 1H), 3.77 (s, 2H), 3.60 (s, 2H), 3.52 (s, 2H), 3.09 (q, J = 7.4 Hz, 2H), 2.35 (t, J = 7.2 Hz, 2H), 1.59–1.43 (m, 2H), 1.24 (s, 3H), 0.81 (t, J = 7.3 Hz, 3H). MS (ESI) m/z: 483.2 [MH+]. ^{13}C NMR (151 MHz, $CDCl_3$) δ 167.79, 141.31, 137.18, 136.45, 131.12, 130.23, 129.35, 128.56, 123.87, 119.83, 115.18, 115.03, 57.77, 55.30, 50.64, 50.51, 44.07, 20.01, 11.75, 7.38. HRMS (m/z): [MH$^+$] calcd for $C_{27}H_{32}FN_2O_3S$ 483.2112; found, 483.2115.

*4.2.1.3. 2-(4-(ethylsulfonyl)phenyl)-N-(4-(((2-methylbenzyl)(propyl)amino)methyl)phenyl)acetamide **(2b)**.* Yield: 77%, white solid. ^{1}H NMR (400 MHz, $CDCl_3$) δ 7.87 (s, 1H), 7.80 (d, J = 8.2 Hz, 2H), 7.48 (d, J = 8.1 Hz, 2H), 7.42 (d, J = 8.3 Hz, 2H), 7.39–7.34 (m, 1H), 7.24 (s, 1H), 7.18–7.08 (m, 3H), 3.73 (s, 2H), 3.48 (d, J = 11.5 Hz, 4H), 3.09 (q, J = 7.4 Hz, 2H), 2.38–2.27 (m, 5H), 1.50 (dd, J = 14.5, 7.2 Hz, 2H), 1.26–1.22 (m, 3H), 0.80 (t, J = 7.3 Hz, 3H). MS (ESI) m/z: 479.2 [MH+]. ^{13}C NMR (151 MHz, $CDCl_3$) δ 167.73, 141.29, 137.14, 130.22, 130.15, 129.58, 129.39, 128.54, 126.75, 125.53, 119.72, 57.97, 56.65, 55.72, 50.64, 44.05, 29.69, 19.34, 11.86. HRMS (m/z): [MH$^+$] calcd for $C_{28}H_{35}N_2O_3S$ 479.2363; found, 479.2376.

*4.2.1.4. N-(4-(((2-chlorobenzyl)(propyl)amino)methyl)phenyl)-2-(4-(ethylsulfonyl)phenyl)acetamide **(2c)**.* Yield: 46%, white solid. ^{1}H NMR (400 MHz, $CDCl_3$) δ 7.85 (d, J = 8.1 Hz, 2H), 7.54 (d, J = 8.0 Hz, 2H), 7.44 (d, J = 7.1 Hz, 2H), 7.37–7.27 (m, 3H), 7.22 (d, J = 7.2 Hz, 1H), 7.17 (d, J = 7.5 Hz, 2H), 3.80 (s, 2H), 3.76–3.44 (m, 4H), 3.10 (q, J = 7.3 Hz, 2H), 2.51–2.34 (m, 2H), 1.66–1.45 (m, 2H), 1.29–1.26 (m, 3H), 0.82 (t, J = 7.3 Hz, 3H). MS (ESI) m/z: 499.1 [MH+]. ^{13}C NMR (151 MHz, $CDCl_3$) δ 167.85, 141.20, 137.34, 134.19, 130.29, 129.73, 129.45, 128.65, 126.88, 119.88, 57.73, 55.32, 54.64, 50.64, 44.15, 29.70, 11.69, 7.41. HRMS (m/z): [MH$^+$] calcd for $C_{27}H_{32}ClN_2O_3S$ 499.1817; found, 499.1819.

*4.2.1.5. N-(4-(((3-chlorobenzyl)(propyl)amino)methyl)phenyl)-2-(4-(ethylsulfonyl)phenyl)acetamide **(2d)**.* Yield: 51%, white solid. ^{1}H NMR (400 MHz, $CDCl_3$) δ 7.81 (d, J = 8.2 Hz, 2H), 7.79 (s, 1H), 7.50 (d, J = 8.1 Hz, 2H), 7.44 (d, J = 8.3 Hz, 2H), 7.33 (s, 1H), 7.27 (d, J = 9.8 Hz, 2H), 7.20 (s, 2H), 3.76 (s, 2H), 3.47 (d, J = 2.5 Hz, 4H), 3.09 (q, J = 7.4 Hz, 2H), 2.33 (t, J = 7.2 Hz, 2H), 1.54–1.44 (m, 2H), 1.25–1.22 (m, 3H), 0.82 (t, J = 7.3 Hz, 3H). MS (ESI) m/z: 499.1 [MH+]. ^{13}C NMR (151 MHz, $CDCl_3$) δ 167.75, 141.23, 137.24, 136.46, 134.06, 130.23, 129.44, 129.38, 128.69, 128.59, 127.01, 127.01, 126.84, 126.84, 119.85, 57.71, 57.60, 55.33, 50.65, 44.10, 29.69, 11.76, 7.39. HRMS (m/z): [MH$^+$] calcd for $C_{25}H_{32}ClN_2O_3S$ 499.1817; found, 499.1820.

*4.2.1.6. N-(4-(((4-chlorobenzyl)(propyl)amino)methyl)phenyl)-2-(4-(ethylsulfonyl)phenyl)acetamide **(2e)**.* Yield: 80%, white solid. ^{1}H NMR (400 MHz, $CDCl_3$) δ 8.20 (s, 1H), 7.78 (d, J = 8.1 Hz, 2H), 7.51–7.41 (m, 4H), 7.26–7.20 (m, 6H), 3.73 (s, 2H), 3.45 (s, 4H), 3.07 (q, J = 7.4 Hz, 2H), 2.31 (t, J = 7.2 Hz, 2H), 1.55–1.40 (m, 2H), 1.25–1.18 (m, 3H), 0.81 (t, J = 7.3 Hz, 3H).MS (ESI) m/z: 499.1 [MH+]. ^{13}C NMR (151 MHz, $CDCl_3$) δ 167.83, 141.34, 137.16, 136.52, 132.40, 130.23, 130.04, 129.33, 128.53, 128.28, 119.83, 57.65, 57.40, 55.25, 50.64, 44.04, 29.69, 11.76, 7.38. HRMS (m/z): [MH$^+$] calcd for $C_{27}H_{32}ClN_2O_3S$ 499.1817; found, 499.1825.

*4.2.1.7. N-(4-(((cyclopropylmethyl)(propyl)amino)methyl)phenyl)-2-(4-(ethylsulfonyl)phenyl)acetamide **(3a)**.* Yield: 78%, white solid. ^{1}H NMR (400 MHz, $CDCl_3$) δ 7.85 (d, J = 8.2 Hz, 2H), 7.59 (d, J = 8.2 Hz, 2H), 7.55 (d, J = 9.1 Hz, 2H), 7.37 (d, J = 8.2 Hz, 2H), 3.86 (s, 2H), 3.77 (s, 2H), 3.11 (q, J = 7.4 Hz, 2H), 2.68–2.57 (m, 2H), 2.50 (d, J = 6.1 Hz, 2H), 1.57 (dt, J = 14.6, 7.3 Hz, 2H), 1.30–1.26 (m, 3H), 0.87 (t, J = 7.3 Hz, 4H), 0.55 (d, J = 7.7 Hz, 2H), 0.14 (d, J = 4.7 Hz, 2H), 0.07 (s, 1H). MS (ESI) m/z: 429.2 [MH+]. ^{13}C NMR (151 MHz, $CDCl_3$) δ 168.01, 165.79, 141.75, 137.15, 136.69, 130.24, 129.25, 128.50, 119.66, 58.81, 56.25, 50.67, 38.63, 31.82, 26.19, 11.86, 7.41. HRMS (m/z): [MH$^+$] calcd for $C_{27}H_{39}N_2O_3S$ 471.2676; found, 471.2681.

*4.2.1.8. N-(4-(((cyclobutylmethyl)(propyl)amino)methyl)phenyl)-2-(4-(ethylsulfonyl)phenyl)acetamide **(3b)**.* Yield: 36%, white solid. ^{1}H NMR (400 MHz, $CDCl_3$) δ 7.80 (d, J = 7.8 Hz, 2H), 7.51 (s, 1H), 7.47 (d, J = 7.9 Hz, 2H), 7.35 (d, J = 7.9 Hz, 2H), 7.18 (d, J = 16.4 Hz, 2H), 3.72 (s, 2H), 3.41 (s, 2H), 3.05 (q, J = 7.3 Hz, 2H), 2.51–2.39 (m, 1H), 2.25 (t, J = 6.9 Hz, 2H), 1.98–1.88 (m, 2H), 1.78 (dd, J = 17.7, 8.6 Hz, 3H), 1.60–1.45 (m, 2H), 1.42–1.32 (m, 2H), 1.24–1.20 (m, 3H), 0.75 (t, J = 7.1 Hz, 3H). MS (ESI) m/z: 443.2 [MH+]. ^{13}C NMR (151 MHz, $CDCl_3$) δ 167.70, 141.13, 137.43, 130.30, 129.62, 128.70, 119.75, 59.85, 58.17, 55.65, 50.65, 44.21, 33.50, 27.50, 18.73, 11.76, 7.42, 1.02. HRMS (m/z): [MH$^+$] calcd for $C_{25}H_{35}N_2O_3S$ 443.2363; found, 443.2375.

*4.2.1.9. N-(4-(((cyclopentylmethyl)(propyl)amino)methyl)phenyl)-2-(4-(ethylsulfonyl)phenyl)acetamide **(3c)**.* Yield: 83%, white solid. ^{1}H NMR (400 MHz, $CDCl_3$) δ 9.59 (s, 1H), 7.81 (d, J = 7.9 Hz, 2H), 7.64 (d, J = 7.6 Hz, 2H), 7.57 (d, J = 7.9 Hz, 2H), 7.30 (d, J = 7.9 Hz, 2H), 4.13 (s, 2H), 3.83 (s, 2H), 3.48 (s, 2H), 3.10 (q, J = 7.3 Hz, 2H), 3.00–2.90 (m, 2H), 1.83 (d, J = 17.9 Hz, 2H), 1.81–1.69 (m, 2H), 1.67–1.45 (m, 4H), 1.26 (t, J = 7.4 Hz, 3H), 1.13 (d, J = 7.8 Hz, 2H), 0.90 (t, J = 7.1 Hz, 3H). MS (ESI) m/z: 457.2 [MH+]. ^{13}C NMR (151 MHz, $CDCl_3$) δ 168.89, 141.63, 140.19, 137.06, 131.56, 130.32, 128.44, 123.80, 120.33, 57.27, 57.17, 53.69, 50.63, 43.81, 35.27, 31.79, 31.65, 24.90, 24.85, 16.52, 11.01, 7.40. HRMS (m/z): [MH$^+$] calcd for $C_{26}H_{37}N_2O_3S$ 457.2519; found, 457.2537.

*4.2.1.10. N-(4-(((cyclohexylmethyl)(propyl)amino)methyl)phenyl)-2-(4-(ethylsulfonyl)phenyl)acetamide **(3d)**.* Yield: 89%, white solid. ^{1}H NMR (400 MHz, $CDCl_3$) δ 7.92 (d, J = 8.7 Hz, 2H), 7.85 (d, J = 8.0 Hz, 2H), 7.70 (d, J = 7.8 Hz, 2H), 7.69–7.61 (m, 2H), 4.02 (s, 2H), 3.10 (dd, J = 14.9, 7.5 Hz, 3H), 2.00 (M, 1H), 1.92–1.83 (m, 1H), 1.77 (d, J = 10.5 Hz, 2H), 1.34–1.26 (m, 8H), 0.99 (M, 4H), 0.93–0.85 (m, 3H), 0.10–0.05 (m, 5H). MS (ESI) m/z: 471.2 [MH+]. ^{13}C NMR (151 MHz, $CDCl_3$) δ 168.20, 141.51, 137.66, 137.18, 130.33, 130.07, 128.54, 119.91, 58.00, 57.64, 54.77, 50.65, 44.06, 18.89, 11.67, 7.41, 7.27, 4.25, 1.02. HRMS (m/z): [MH$^+$] calcd for $C_{24}H_{33}N_2O_3S$ 429.2206; found, 429.2211.

*4.2.1.11. N-(4-((((4,4-difluorocyclohexyl)methyl)(propyl)amino)methyl)phenyl)-2-(4-(ethylsulfonyl)phenyl)acetamide **(3e)**.* Yield: 87%, white solid. ^{1}H NMR (400 MHz, $CDCl_3$) δ 7.88 (d, J = 8.2 Hz, 2H), 7.55 (d, J = 8.1 Hz, 2H), 7.41 (d, J = 8.2 Hz, 2H), 7.25 (d, J = 3.4 Hz, 2H), 3.80 (s, 2H), 3.73–3.69 (m, 1H), 3.47 (s, 2H), 3.11 (q,

J = 7.4 Hz, 3H), 2.20 (d, J = 6.7 Hz, 2H), 2.00 (s, 3H), 1.86 (t, J = 12.0 Hz, 3H), 1.25 (d, J = 8.3 Hz, 5H), 0.84 (dd, J = 13.6, 6.4 Hz, 4H). MS (ESI) m/z: 507.2 [MH+]. ^{13}C NMR (101 MHz, $CDCl_3$) δ 130.34 (s), 128.69 (s), 119.87 (s), 58.80 (s), 56.35 (s), 50.65 (s), 44.19 (s), 33.09 (s), 29.70 (s), 29.33 (s), 27.44 (d, J = 8.6 Hz), 22.70 (s), 11.63 (s), 7.42 (s). HRMS (m/z): [MH^+] calcd for $C_{27}H_{36}F_2N_2O_3S$ 507.2487; found, 507.2487.

4.2.1.12. 2-(4-(ethylsulfonyl)phenyl)-N-(4-((propyl((tetrahydro-2H-pyran-4-yl)methyl)amino)methyl)phenyl)acetamide ***(3f)***. Yield: 55%, white solid. ^{1}H NMR (400 MHz, $CDCl_3$) δ 7.88 (d, J = 8.0 Hz, 2H), 7.55 (d, J = 7.7 Hz, 2H), 7.40 (d, J = 8.6 Hz, 2H), 7.23 (d, J = 7.7 Hz, 2H), 3.90 (d, J = 10.9 Hz, 2H), 3.80 (s, 2H), 3.47 (s, 2H), 3.34 (t, J = 11.2 Hz, 2H), 3.19−3.04 (m, 2H), 2.38−2.26 (m, 2H), 2.23−2.16 (m, 2H), 1.48−1.40 (m, 2H), 1.26 (d, J = 6.9 Hz, 3H), 1.12 (m, 3H), 0.83 (t, J = 7.3 Hz, 3H).MS (ESI) m/z: 473.2 [MH+]. ^{13}C NMR (151 MHz, $CDCl_3$) δ 167.53, 141.04, 137.47, 130.32, 129.79, 128.72, 119.81, 67.77, 58.71, 56.23, 50.64, 44.19, 31.53, 29.71, 11.70, 7.42, 1.02. HRMS (m/z): [MH^+] calcd for $C_{26}H_{37}N_2O_4S$ 473.2469; found, 473.2474.

4.2.1.13. 2-(4-(ethylsulfonyl)phenyl)-N-(4-((propyl((tetrahydrofuran-2-yl)methyl)amino)methyl)phenyl)acetamide ***(3g)***. Yield: 67%, white solid. ^{1}H NMR (400 MHz, $CDCl_3$) δ 7.86 (d, J = 8.1 Hz, 2H), 7.53 (d, J = 8.1 Hz, 2H), 7.41 (d, J = 8.3 Hz, 2H), 7.26 (d, J = 4.4 Hz, 2H), 3.99 (dd, J = 12.8, 6.4 Hz, 1H), 3.80 (s, 1H), 3.77 (s, 2H), 3.74−3.70 (m, 2H), 3.11 (q, J = 7.4 Hz, 3H), 2.46−2.36 (m, 2H), 2.00−1.86 (m, 2H), 1.80 (dt, J = 13.4, 6.8 Hz, 3H), 1.52−1.41 (m, 3H), 1.26−1.24 (m, 3H), 0.82 (t, J = 7.3 Hz, 3H). MS (ESI) m/z: 459.2 [MH+]. ^{13}C NMR (151 MHz, $CDCl_3$) δ 167.81, 141.15, 137.39, 130.29, 129.98, 128.67, 119.76, 68.15, 58.38, 57.40, 55.87, 50.65, 44.15, 30.29, 25.32, 19.41, 11.65, 7.42. HRMS (m/z): [MH^+] calcd for $C_{25}H_{35}N_2O_4S$ 459.2312; found, 459.2318.

4.2.1.14. 4-((benzyl(propyl)amino)methyl)-N-(4-(ethylsulfonyl) benzyl)benzamide ***(6b)***. Yield: 80%, white solid. ^{1}H NMR (400 MHz, $CDCl_3$) δ 7.81 (d, J = 8.0 Hz, 2H), 7.77 (d, J = 8.1 Hz, 2H), 7.48 (dd, J = 14.5, 8.0 Hz, 4H), 7.38−7.33 (m, 2H), 7.30 (t, J = 7.4 Hz, 2H), 7.25−7.20 (m, 1H), 6.79 (s, 1H), 4.72 (s, 2H), 3.58 (d, J = 11.4 Hz, 4H), 3.08 (q, J = 7.4 Hz, 2H), 2.38 (t, J = 7.0 Hz, 2H), 1.53 (dd, J = 14.1, 7.2 Hz, 2H), 1.25 (t, J = 7.4 Hz, 3H), 0.84 (t, J = 7.3 Hz, 3H). MS (ESI) m/z: 465.2 [MH+]. ^{13}C NMR (151 MHz, $CDCl_3$) δ 167.61, 145.19, 137.08, 132.30, 128.87, 128.71, 128.43, 128.20, 128.12, 127.03, 126.70, 58.33, 57.95, 55.54, 50.63, 43.17, 20.15, 11.79, 7.38. HRMS (m/z): [MH^+] calcd for $C_{27}H_{33}N_2O_3S$ 465.2206; found, 465.2211.

4.2.1.15. 4-((benzyl(propyl)amino)methyl)-N-(4-(ethylsulfonyl)phenethyl)aniline ***(6c)***. A mixture of *N*-(4-((benzyl(propyl)amino) methyl)phenyl)-2-(4-(ethylsulfonyl)phenyl)acetamide (**1**) (80 mg, 0.17 mmol) and BH_3 in THF (0.5 mL, 0.5 mmol) was stirred under ice bath for 30 min, and was then stirred overnight at room temperature. Purification through pTLC (PE:EA 1:1) afforded white solid (50 mg, yield: 65%). ^{1}H NMR (400 MHz, $CDCl_3$) δ 7.83 (d, J = 8.1 Hz, 2H), 7.40 (d, J = 8.0 Hz, 2H), 7.36 (d, J = 7.3 Hz, 2H), 7.29 (t, J = 7.3 Hz, 2H), 7.21 (d, J = 8.5 Hz, 1H), 7.17 (d, J = 8.1 Hz, 2H), 6.56 (d, J = 8.2 Hz, 2H), 3.56 (s, 2H), 3.48 (d, J = 5.9 Hz, 2H), 3.42 (t, J = 6.8 Hz, 2H), 3.10 (q, J = 7.4 Hz, 2H), 2.99 (t, J = 6.7 Hz, 2H), 2.37 (t, J = 6.8 Hz, 2H), 1.53 (dd, J = 14.3, 7.2 Hz, 2H), 1.27 (t, J = 7.5 Hz, 3H), 0.83 (t, J = 7.3 Hz, 3H). MS (ESI) m/z: 451.2 [MH+]. ^{13}C NMR (151 MHz, $CDCl_3$) δ 146.43, 146.09, 136.60, 130.05, 129.67, 128.81, 128.51, 128.09, 126.68, 112.76, 57.95, 57.59, 55.08, 50.62, 44.78, 35.54, 20.01, 11.82, 7.46. HRMS (m/z): [MH^+] calcd for $C_{27}H_{35}N_2O_2S$ 451.2414; found, 451.2411.

4.2.2. General procedure B for the synthesis of compounds (2f-2h, 4b-4g, 5a-5c, 6a, 7a-7e, 8a-8c)

Step 1. To a solution of aldehyde (1.0 eq) and alkylamine (1.1 eq) in dry DCM was added Na_2SO_4 and stirred overnight. The mixture was filtered and evaporated under reduced pressure. Then, the residue was re-dissolved in methanol, carefully added $NaBH_4$ (0.5 eq) under ice bath and was stirred for 1 h at room temperature. The reaction was quenched by saturated Na_2CO_3, extracted with EA and dried over Na_2SO_4. The combined organic phase was evaporated to afford the desired intermediate **16**.

Step 2. A mixture of intermediate **16** (1.0 eq), nitrobenzene intermediates (0.5 eq), anhydrous potassium carbonate (1.5 eq) and acetonitrile was heated up to reflux for 4 h. The solvent was removed. The residue was re-dissolved, washed with brine and dried over Na_2SO_4. Purification by column chromatography through silica gel afforded intermediate **17**.

Step 3. To a solution of intermediate **17** (1.0 eq) in methanol was added Adams' catalyst. The mixture was degassed and purged with hydrogen and stirred at room temperature for 1 h. The solution was filtered through celite and evaporated to afford desired amine **18**.

Step 4. To a solution of **18** (1.0 eq) in DCM was added *p*-alkylsulfone aryl acetic acid (1.2 eq), HATU (1.2 eq) and DIPEA (1.2 eq). The mixture was stirred at room temperature for 5 h. Purification by column chromatography through silica gel afforded desired compound (**2f-2h, 4b-4g, 5a-5c, 6a, 7a-7e, 8a-8c**)

4.2.2.1. 2-(4-(ethylsulfonyl)phenyl)-N-(4-((propyl(thiophen-2-ylmethyl)amino)methyl)phenyl)acetamide ***(2f)***. Yield: 78%, white solid. ^{1}H NMR (400 MHz, $CDCl_3$) δ 7.84 (d, J = 10.5 Hz, 2H), 7.80 (s, 1H), 7.56 (d, J = 7.5 Hz, 2H), 7.47 (d, J = 8.1 Hz, 2H), 7.33 (d, J = 7.8 Hz, 2H), 7.22 (s, 1H), 6.98−6.84 (m, 2H), 3.81 (s, 4H), 3.59 (s, 2H), 3.10 (d, J = 6.3 Hz, 3H), 2.43 (s, 2H), 1.30−1.26 (m, 3H), 0.88−0.80 (m, 3H). MS (ESI) m/z: 471.2 [MH+]. ^{13}C NMR (151 MHz, $CDCl_3$) δ 168.37, 141.46, 137.16, 130.37, 130.27, 128.53, 127.06, 120.10, 57.08, 54.49, 50.63, 44.00, 29.71, 11.42, 7.40. HRMS (m/z): [MH^+] calcd for $C_{25}H_{31}N_2O_3S_2$ 471.1771; found, 471.1775.

4.2.2.2. 2-(4-(ethylsulfonyl)phenyl)-N-(4-((propyl(pyridin-2-ylmethyl)amino)methyl)phenyl)acetamide ***(2g)***. Yield: 65%, white solid. The title compound was synthesized following the procedure for compound **2f**. ^{1}H NMR (400 MHz, $CDCl_3$) δ 8.46 (s, 1H), 8.00 (s, 1H), 7.82 (d, J = 6.9 Hz, 2H), 7.65 (s, 1H), 7.55−7.46 (m, 3H), 7.43 (d, J = 7.1 Hz, 2H), 7.27 (s, 1H), 7.14 (s, 1H), 3.74 (d, J = 16.5 Hz, 4H), 3.59 (s, 2H), 3.09 (d, J = 6.5 Hz, 2H), 2.43 (s, 3H), 1.58−1.45 (m, 2H), 1.27 (s, 1H), 0.92−0.78 (m, 4H). MS (ESI) m/z: 466.2 [MH+]. ^{13}C NMR (151 MHz, $CDCl_3$) δ 168.09, 148.73, 141.44, 137.10, 136.79, 130.29, 129.68, 128.49, 123.03, 122.32, 119.95, 59.24, 58.04, 55.83, 50.63, 43.94, 19.79, 11.64, 7.38. HRMS (m/z): [MH^+] calcd for $C_{26}H_{32}N_3O_3S$ 466.2159; found, 466.2167.

4.2.2.3. 2-(4-(ethylsulfonyl)phenyl)-N-(4-((propyl(thiazol-2-ylmethyl)amino)methyl)phenyl)acetamide ***(2h)***. Yield: 65%, white solid. ^{1}H NMR (400 MHz, $CDCl_3$) δ 7.89 (d, J = 7.8 Hz, 2H), 7.68 (s, 1H), 7.55 (d, J = 7.8 Hz, 2H), 7.48−7.41 (m, 2H), 7.40−7.31 (m, 3H), 3.91 (s, 2H), 3.80 (s, 2H), 3.65 (s, 2H), 3.11 (d, J = 7.3 Hz, 2H), 2.48 (s, 2H), 1.62 (s, 1H), 1.31−1.27 (m, 3H), 0.86 (t, J = 7.1 Hz, 4H). MS (ESI) m/z: 472.2 [MH+]. ^{13}C NMR (151 MHz, $CDCl_3$) δ 172.57, 167.86, 142.13, 141.36, 137.12, 136.76, 135.21, 130.19, 129.31, 128.50, 119.89, 119.38, 57.96, 55.79, 55.23, 50.64, 43.99, 20.30, 11.68, 7.38. HRMS (m/z): [MH^+] calcd for $C_{24}H_{30}N_3O_3S_2$ 472.1723; found, 472.1729.

4.2.2.4. N-(4-((benzyl(methyl)amino)methyl)phenyl)-2-(4-(ethylsulfonyl)phenyl)acetamide ***(4b)***. Yield: 77%, white solid. ^{1}H NMR (400 MHz, $CDCl_3$) δ 8.08 (s, 1H), 7.84 (d, J = 7.8 Hz, 2H), 7.59 (d, J = 7.8 Hz, 2H), 7.52 (s, 1H), 7.50 (d, J = 8.0 Hz, 3H), 7.29 (d, J = 10.4 Hz,

5H), 3.81 (s, 2H), 3.68–3.64 (m, 4H), 3.14 (d, J = 7.1 Hz, 4H), 2.24 (d, J = 11.1 Hz, 4H).MS (ESI) m/z: 437.2 [MH+]. ^{13}C NMR (151 MHz, $CDCl_3$) δ 168.92, 141.66, 137.71, 136.43, 134.32, 130.50, 130.32, 130.15, 129.56, 128.49, 128.18, 127.97, 120.38, 55.29, 43.20, 17.33, 12.41, 6.99. HRMS (m/z): [MH^+] calcd for $C_{25}H_{29}N_2O_3S$ 437.1893; found, 437.1891.

4.2.2.5. N-(4-((benzyl(ethyl)amino)methyl)phenyl)-2-(4-(ethylsulfonyl)phenyl)acetamide ***(4c)***. Yield: 40%, white solid. ^{1}H NMR (400 MHz, $CDCl_3$) δ 7.85 (d, J = 8.2 Hz, 2H), 7.69 (s, 1H), 7.56 (d, J = 8.1 Hz, 2H), 7.45 (d, J = 8.4 Hz, 2H), 7.34 (t, J = 6.5 Hz, 3H), 7.31–7.26 (m, 4H), 3.80 (s, 2H), 3.61 (s, 2H), 3.13 (dd, J = 13.8, 6.3 Hz, 4H), 3.08 (d, J = 7.4 Hz, 2H), 1.08 (t, J = 7.1 Hz, 3H). MS (ESI) m/z: 451.2 [MH+]. ^{13}C NMR (151 MHz, $CDCl_3$) δ 169.01, 141.88, 137.40, 136.67, 136.23, 130.53, 129.90, 129.32, 128.57, 128.24, 127.87, 120.58, 57.23, 56.89, 55.58, 43.49, 17.58, 12.66, 7.26. HRMS (m/z): [MH^+] calcd for $C_{26}H_{31}N_2O_3S$ 451.2050; found, 451.2053.

4.2.2.6. N-(4-((benzyl(isobutyl)amino)methyl)phenyl)-2-(4-(ethylsulfonyl)phenyl)acetamide ***(4d)***. Yield: 60%, white solid. ^{1}H NMR (400 MHz, $CDCl_3$) δ 7.85 (t, J = 7.2 Hz, 2H), 7.55 (t, J = 7.4 Hz, 2H), 7.45 (t, J = 6.5 Hz, 2H), 7.37–7.27 (m, 6H), 7.23 (s, 1H), 3.79 (d, J = 7.0 Hz, 2H), 3.53–3.44 (m, 3H), 3.19–3.01 (m, 2H), 2.83–2.81 (m, 7H), 2.12 (s, 2H), 1.32–1.23 (m, 4H). MS (ESI) m/z: 479.2 [MH+]. ^{13}C NMR (151 MHz, $CDCl_3$) δ 167.89, 141.51, 139.89, 137.17, 136.54, 130.22, 129.35, 128.81, 128.51, 128.10, 126.74, 58.69, 58.22, 50.65, 44.02, 38.64, 26.07, 20.78, 14.19, 7.38. HRMS (m/z): [MH^+] calcd for $C_{28}H_{35}N_2O_3S$ 479.2363; found, 479.2360.

4.2.2.7. N-(4-((benzyl(cyclopropylmethyl)amino)methyl)phenyl)-2-(4-(ethylsulfonyl)phenyl)acetamide ***(4e)***. Yield: 83%, white solid. ^{1}H NMR (400 MHz, $CDCl_3$) δ 7.86 (d, J = 8.0 Hz, 2H), 7.53 (d, J = 7.7 Hz, 2H), 7.41 (d, J = 8.0 Hz, 2H), 7.37–7.27 (m, 6H), 7.21 (d, J = 7.5 Hz, 1H), 3.78 (s, 2H), 3.61 (d, J = 11.2 Hz, 4H), 3.10 (q, J = 7.4 Hz, 2H), 2.82–2.76 (m, 3H), 2.29 (d, J = 5.6 Hz, 2H), 1.29–1.26 (m, 3H), 0.44 (d, J = 7.3 Hz, 2H). MS (ESI) m/z: 477.2 [MH+]. ^{13}C NMR (151 MHz, $CDCl_3$) δ 168.12, 141.32, 139.04, 136.25, 136.03, 135.23, 129.59, 128.61, 128.11, 127.59, 127.48, 126.12, 119.29, 57.52, 57.32, 56.90, 49.34, 42.93, 37.86, 7.57, 6.57, 3.31. HRMS (m/z): [MH^+] calcd for $C_{28}H_{33}N_2O_3S$ 477.2206; found, 477.2205.

4.2.2.8. N-(4-((benzyl(butyl)amino)methyl)phenyl)-2-(4-(ethylsulfonyl)phenyl)acetamide ***(4f)***. Yield: 45%, white solid. ^{1}H NMR (400 MHz, $CDCl_3$) δ 7.85 (d, J = 7.8 Hz, 2H), 7.58–7.46 (m, 3H), 7.41 (d, J = 8.2 Hz, 2H), 7.34–7.26 (m, 5H), 7.22–7.15 (m, 1H), 3.77 (s, 2H), 3.50 (d, J = 11.8 Hz, 4H), 3.15–3.01 (m, 2H), 2.81–2.75 (m, 5H), 2.37 (s, 2H), 1.25–1.23 (m, 2H), 0.82–0.74 (m, 3H). MS (ESI) m/z: 479.2 [MH+]. ^{13}C NMR (151 MHz, $CDCl_3$) δ 167.65, 141.21, 139.67, 137.34, 136.29, 130.24, 129.38, 58.13, 57.67, 50.66, 44.15, 38.65, 29.11, 20.45, 14.02, 7.40. HRMS (m/z): [MH^+] calcd for $C_{28}H_{35}N_2O_3S$ 479.2363; found, 479.2369.

4.2.2.9. N-(4-((benzyl(cyclobutylmethyl)amino)methyl)phenyl)-2-(4-(ethylsulfonyl)phenyl)acetamide ***(4g)***. Yield: 76%, white solid. ^{1}H NMR (400 MHz, $CDCl_3$) δ 8.10 (s, 1H), 7.79 (d, J = 8.0 Hz, 2H), 7.48 (t, J = 8.4 Hz, 2H), 7.43 (d, J = 8.1 Hz, 2H), 7.29 (dd, J = 12.0, 5.3 Hz, 3H), 7.26–7.22 (m, 3H), 7.20 (d, J = 6.9 Hz, 1H), 3.73 (s, 2H), 3.44 (d, J = 13.1 Hz, 4H), 3.07 (q, J = 7.4 Hz, 2H), 2.79 (s, 4H), 2.38 (d, J = 7.0 Hz, 2H), 1.81 (dd, J = 18.3, 8.9 Hz, 1H), 1.23 (d, J = 7.2 Hz, 5H). MS (ESI) m/z: 491.2 [MH+]. ^{13}C NMR (151 MHz, $CDCl_3$) δ 167.61, 141.16, 137.37, 130.24, 129.35, 128.74, 128.65, 128.13, 126.79, 59.88, 58.41, 57.92, 50.66, 44.17, 38.64, 33.76, 27.31, 18.69, 7.40. HRMS (m/z): [MH^+] calcd for $C_{29}H_{35}N_2O_3S$ 491.2363; found, 491.2359.

4.2.2.10. N-(4-((benzyl(propyl)amino)methyl)-3-chlorophenyl)-2-(4-(ethylsulfonyl)phenyl)acetamide ***(5a)***. Yield: 47%, white solid. ^{1}H NMR (400 MHz, $CDCl_3$) δ 8.01 (s, 1H), 7.78 (d, J = 8.2 Hz, 2H), 7.61 (s, 1H), 7.53 (d, J = 8.4 Hz, 1H), 7.46 (d, J = 8.1 Hz, 2H), 7.33 (d, J = 3.1 Hz, 1H), 7.30–7.23 (m, 3H), 7.20 (t, J = 7.1 Hz, 1H), 3.73 (s, 2H), 3.57 (d, J = 13.5 Hz, 4H), 3.09 (q, J = 7.4 Hz, 2H), 2.36 (t, J = 7.2 Hz, 2H), 1.57–1.44 (m, 2H), 1.25 (t, J = 7.4 Hz, 3H), 0.81 (t, J = 7.3 Hz, 3H). MS (ESI) m/z: 499.2 [MH+]. ^{13}C NMR (151 MHz, $CDCl_3$) δ 168.22, 141.36, 139.70, 137.24, 136.95, 133.98, 133.56, 130.63, 130.20, 128.65, 128.37, 128.13, 126.78, 120.53, 118.22, 58.42, 55.72, 54.66, 50.64, 43.77, 20.10, 11.82, 7.32. HRMS (m/z): [MH^+] calcd for $C_{27}H_{32}ClN_2O_3S$ 499.1817; found, 499.1820.

4.2.2.11. N-(4-((benzyl(cyclopropylmethyl)amino)methyl)-3-chlorophenyl)-2-(4-(ethylsulfonyl)phenyl)acetamide ***(5b)***. Yield: 38%, white solid. ^{1}H NMR (400 MHz, $CDCl_3$) δ 8.06 (s, 1H), 7.79 (d, J = 8.0 Hz, 2H), 7.63 (s, 1H), 7.58 (d, J = 8.4 Hz, 1H), 7.47 (d, J = 8.0 Hz, 2H), 7.37 (s, 1H), 7.32 (d, J = 13.4 Hz, 1H), 7.27 (d, J = 8.9 Hz, 2H), 7.21 (t, J = 7.2 Hz, 1H), 3.74 (s, 2H), 3.71 (s, 2H), 3.67 (s, 2H), 3.10 (q, J = 7.4 Hz, 2H), 2.33 (d, J = 6.4 Hz, 2H), 1.26 (t, J = 7.4 Hz, 3H), 0.97–0.85 (m, 1H), 0.45 (q, J = 4.8 Hz, 2H), 0.05–0.00 (m, 2H). MS (ESI) m/z: 511.2 [MH+]. ^{13}C NMR (151 MHz, $CDCl_3$) δ 168.28 (s), 141.39 (s), 139.76 (s), 137.24 (s), 136.89 (s), 133.95 (s), 133.55 (s), 130.64 (s), 130.21 (s), 128.58 (s), 128.33 (s), 128.13 (s), 126.77 (s), 120.54 (s), 118.24 (s), 58.55 (s), 58.26 (s), 54.42 (s), 50.63 (s), 43.73 (s), 8.35 (s), 7.30 (s), 3.96 (s).

4.2.2.12. N-(4-((benzyl(propyl)amino)methyl)-3,5-dichlorophenyl)-2-(4-(ethylsulfonyl)phenyl)acetamide ***(5c)***. Yield: 71%, white solid. ^{1}H NMR (400 MHz, $CDCl_3$) δ 8.19 (s, 1H), 7.77 (d, J = 8.3 Hz, 2H), 7.55 (s, 2H), 7.45 (d, J = 8.3 Hz, 2H), 7.27 (t, J = 5.8 Hz, 2H), 7.23 (t, J = 7.3 Hz, 2H), 7.20–7.15 (m, 1H), 3.80 (s, 2H), 3.74 (s, 2H), 3.54 (s, 2H), 3.11 (q, J = 7.4 Hz, 2H), 2.37 (dd, J = 8.2, 6.5 Hz, 2H), 1.58–1.44 (m, 2H), 1.26 (dd, J = 7.7, 4.7 Hz, 3H), 0.76 (t, J = 7.3 Hz, 3H). MS (ESI) m/z: 533.1 [MH+]. ^{13}C NMR (151 MHz, $CDCl_3$) δ 168.27, 141.04, 140.02, 137.83, 137.11, 137.01, 130.99, 130.21, 128.79, 128.44, 127.90, 126.62, 119.33, 57.92, 55.48, 53.12, 50.70, 43.83, 19.41, 11.88, 7.33. HRMS (m/z): [MH^+] calcd for $C_{27}H_{31}Cl_2N_2O_3S$ 533.1427; found, 533.1435.

4.2.2.13. 1-(4-((benzyl(propyl)amino)methyl)phenyl)-3-(4-(ethylsulfonyl)benzyl)urea ***(6a)***. A mixture of 4-((benzyl(propyl)amino) methyl)aniline (90 mg, 0.35 mmol), triphosgene (35 mg, 0.12 mmol) and DIPEA (181 μL, 1.05 mmol) in dry DCM (1 mL) was stirred under ice bath for 30 min, then (4-(ethylsulfonyl)phenyl) methanamine (70 mg, 0.35 mmol) was added. The mixture was stirred at room temperature overnight. Purification by column chromatography (DCM:MeOH 50:1) through silica gel afforded white solid (90 mg, yield: 53.7%). ^{1}H NMR (400 MHz, $CDCl_3$) δ 7.69 (s, 1H), 7.65 (d, J = 8.2 Hz, 2H), 7.35–7.27 (m, 6H), 7.25–7.16 (m, 5H), 4.31 (d, J = 5.7 Hz, 2H), 3.49 (s, 2H), 3.43 (s, 2H), 3.03 (q, J = 7.4 Hz, 2H), 2.32 (t, J = 7.2 Hz, 2H), 1.54–1.44 (m, 2H), 1.19 (t, J = 7.4 Hz, 3H), 0.81 (t, J = 7.3 Hz, 3H). MS (ESI) m/z: 480.2 [MH+]. ^{13}C NMR (151 MHz, $CDCl_3$) δ 171.28, 156.21, 146.36, 139.69, 137.55, 136.59, 134.45, 129.42, 128.74, 128.21, 128.14, 127.70, 126.79, 119.59, 58.06, 57.63, 55.23, 50.61, 43.13, 20.01, 11.79, 7.29. HRMS (m/z): [MH^+] calcd for $C_{27}H_{34}N_3O_3S$ 480.2315; found, 480.2317.

4.2.2.14. N-(4-((benzyl(propyl)amino)methyl)phenyl)-2-(4-(methylsulfonyl)phenyl)acetamide ***(7a)***. Yield: 55%, white solid. ^{1}H NMR (400 MHz, $CDCl_3$) δ 9.90 (s, 1H), 7.92 (d, J = 8.1 Hz, 2H), 7.84 (dd, J = 13.1, 8.3 Hz, 2H), 7.71 (d, J = 8.5 Hz, 2H), 7.56 (d, J = 8.0 Hz, 4H), 7.37 (d, J = 6.9 Hz, 3H), 4.02 (s, 2H), 3.86 (s, 2H), 3.05 (s, 3H), 2.80–2.62 (m, 2H), 1.80 (dd, J = 16.7, 8.9 Hz, 4H), 0.90 (t, J = 7.4 Hz, 3H). MS (ESI) m/z: 451.2 [MH+]. ^{13}C NMR (151 MHz, $CDCl_3$) δ 165.78, 141.73, 139.16, 136.81, 130.34, 129.99, 129.25, 128.75, 128.12, 127.66, 127.61,

126.75, 119.76, 58.14, 57.72, 55.29, 44.56, 43.94, 38.63, 11.78. HRMS (*m/z*): [MH$^+$] calcd for $C_{26}H_{31}N_2O_3S$ 451.2050; found, 451.2046.

4.2.2.15. 4-(2-((4-((benzyl(propyl)amino)methyl)phenyl)amino)-2-oxoethyl)benzoic acid ***(7b)***. Yield: 62%, white solid. ^{1}H NMR (400 MHz, CD_3OD) δ 7.95 (d, J = 8.0 Hz, 2H), 7.68 (d, J = 8.3 Hz, 2H), 7.49–7.37 (m, 9H), 4.22 (s, 2H), 4.20 (s, 2H), 3.76 (s, 2H), 2.87 (dd, J = 9.7, 6.6 Hz, 2H), 1.81–1.68 (m, 2H), 0.86 (t, J = 7.3 Hz, 3H). MS (ESI) *m/z*: 415.2 [MH-]. ^{13}C NMR (151 MHz, CD_3OD) δ 169.54, 168.24, 139.42, 139.03, 130.49, 129.95, 129.77, 129.50, 128.76, 128.56, 128.09, 125.21, 119.33, 56.09, 55.79, 52.76, 42.36, 16.24, 9.14. HRMS (*m/z*): [MH$^+$] calcd for $C_{26}H_{29}N_2O_3$ 417.2173; found, 417.2176.

4.2.2.16. N-(4-((benzyl(propyl)amino)methyl)phenyl)-2-(4-cyanophenyl)acetamide ***(7c)***. Yield: 59%, white solid. ^{1}H NMR (400 MHz, $CDCl_3$) δ 7.63 (t, J = 7.8 Hz, 2H), 7.45 (d, J = 8.0 Hz, 2H), 7.40 (d, J = 8.2 Hz, 2H), 7.34 (d, J = 7.4 Hz, 2H), 7.32–7.27 (m, 4H), 7.22 (t, J = 7.2 Hz, 1H), 3.74 (s, 2H), 3.52 (s, 2H), 3.48 (s, 2H), 2.35 (t, J = 7.3 Hz, 2H), 1.52 (dt, J = 14.5, 0.3 Hz, 3H), 0.83 (t, J = 7.3 Hz, 3H). MS (ESI) *m/z*: 398.2 [MH+]. ^{13}C NMR (151 MHz, $CDCl_3$) δ 167.25, 139.75, 139.25, 135.90, 135.66, 131.83, 129.56, 128.69, 128.12, 127.56, 126.18, 119.33, 118.14, 110.40, 57.55, 57.07, 54.72, 43.54, 19.51, 11.22. HRMS (*m/z*): [MH$^+$] calcd for $C_{26}H_{28}N_3O$ 398.2227; found, 398.2236.

4.2.2.17. N-(4-((benzyl(propyl)amino)methyl)phenyl)-2-phenylacetamide ***(7d)***. Yield: 77%, white solid. ^{1}H NMR (400 MHz, $CDCl_3$) δ 7.37 (d, J = 6.5 Hz, 2H), 7.35–7.30 (m, 6H), 7.30 (s, 1H), 7.28 (d, J = 2.5 Hz, 2H), 7.25 (s, 2H), 7.21 (d, J = 7.2 Hz, 1H), 3.71 (s, 2H), 3.50 (s, 2H), 3.47 (s, 2H), 2.37–2.29 (m, 2H), 1.49 (t, J = 14.5, 7.3 Hz, 3H), 0.81 (t, J = 7.3 Hz, 2H). MS (ESI) *m/z*: 373.2 [MH+]. ^{13}C NMR (151 MHz, $CDCl_3$) δ 169.16, 136.37, 134.60, 129.47, 129.24, 129.11, 128.72, 128.10, 127.52, 126.71, 119.70, 58.12, 57.67, 55.27, 44.70, 20.09, 11.77. HRMS (*m/z*): [MH$^+$] calcd for $C_{25}H_{29}N_2O$ 373.2274; found, 373.2277.

4.2.2.18. N-(4-((benzyl(propyl)amino)methyl)phenyl)-2-(5-(ethylsulfonyl)pyridin-2-yl)acetamide ***(7e)***. Yield: 89%, white solid. ^{1}H NMR (400 MHz, $CDCl_3$) δ 10.19 (s, 1H), 8.72 (s, 1H), 7.95 (d, J = 8.0 Hz, 1H), 7.66 (d, J = 8.1 Hz, 2H), 7.57 (d, J = 8.0 Hz, 1H), 7.49 (d, J = 6.9 Hz, 2H), 7.45–7.34 (m, 5H), 4.41–4.30 (m, 2H), 4.30–4.21 (m, 2H), 4.04 (s, 2H), 2.87–2.74 (m, 4H), 1.97–1.86 (m, 2H), 1.22 (t, J = 7.4 Hz, 3H), 0.83 (t, J = 7.2 Hz, 3H). MS (ESI) *m/z*: 466.2 [MH+]. ^{13}C NMR (101 MHz, $CDCl_3$) δ 167.80 (s), 158.59 (s), 145.30 (s), 138.23 (s), 133.22 (d, J = 19.3 Hz), 132.46 (s), 130.21 (s), 128.90 (s), 124.93 (s), 123.17 (s), 119.92 (s), 69.05 (s), 68.84 (s), 63.71 (s), 50.37 (s), 46.18 (s), 29.71 (s), 29.33 (s), 17.20 (s), 14.13 (s), 10.67 (s), 5.96 (s). MS (ESI) *m/z*: 466.2 [MH+]. HRMS (ESI$^+$) *m/z* calcd for $C_{26}H_{31}N_3O_3S$ [M+H]$^+$: 466.2159; found: 466.2163.

4.2.2.19. N-(4-(((cyclohexylmethyl)(propyl)amino)methyl)phenyl)-2-(4-(methylsulfonyl)phenyl)acetamide ***(8a)***. Yield: 48%, white solid. ^{1}H NMR (400 MHz, $CDCl_3$) δ 7.90 (dd, J = 7.3, 4.5 Hz, 2H), 7.55 (dd, J = 7.3, 4.5 Hz, 2H), 7.43 (d, J = 8.4 Hz, 2H), 7.27 (d, J = 8.4 Hz, 2H), 3.79 (s, 2H), 3.50 (s, 2H), 3.04 (s, 3H), 2.33 (t, J = 7.2 Hz, 2H), 2.18 (d, J = 7.0 Hz, 2H), 1.78 (d, J = 12.7 Hz, 2H), 1.70–1.58 (m, 3H), 1.50–1.41 (m, 3H), 1.21–1.05 (m, 3H), 0.83 (t, J = 7.4 Hz, 3H), 0.80–0.70 (m, 2H). MS (ESI) *m/z*: 457.3[MH+]. ^{13}C NMR (101 MHz, $CDCl_3$) δ 167.63 (s), 141.16 (s), 139.43 (s), 136.28 (s), 130.41 (s), 129.51 (s), 127.86 (s), 119.73 (s), 61.03 (s), 58.76 (s), 56.21 (s), 44.55 (s), 44.17 (s), 35.81 (s), 31.77 (s), 26.78 (s), 26.13 (s), 19.91 (s), 11.81 (s). HRMS (*m/z*): [MH$^+$] calcd for $C_{26}H_{36}N_2O_3S$ 457.2519; found, 457.2524.

4.2.2.20. N-(3-chloro-4-(((cyclohexylmethyl)(propyl)amino)methyl)phenyl)-2-(4-(methylsulfonyl)phenyl)acetamide ***(8b)***. Yield: 76%, white solid. ^{1}H NMR (400 MHz, $CDCl_3$) δ 7.92 (d, J = 8.3 Hz, 2H), 7.56 (d, J = 8.2 Hz, 2H), 7.29 (dd, J = 8.4, 2.0 Hz, 1H), 7.26 (s, 2H), 3.82 (s, 2H), 3.62 (s, 2H), 3.06 (s, 3H), 2.39 (s, 2H), 2.22 (d, J = 15.2 Hz, 2H), 1.79 (d, J = 12.4 Hz, 2H), 1.67–1.60 (m, 3H), 1.54–1.42 (m, 3H), 1.21–1.07 (m, 3H), 0.85 (t, J = 7.3 Hz, 3H), 0.82–0.70 (m, 2H). MS (ESI) *m/z*: 490.8[MH+].^{13}C NMR (101 MHz, $CDCl_3$) δ 140.85 (s), 139.58 (s), 130.41 (s), 127.93 (s), 120.47 (s), 118.03 (s), 56.65 (s), 55.71 (s), 44.56 (s), 44.14 (s), 31.82 (s), 26.74 (s), 26.10 (s), 11.85 (s). HRMS (*m/z*): [MH$^+$] calcd for $C_{26}H_{35}ClN_2O_3S$ 491.2130; found, 491.2132.

4.2.2.21. N-(3,5-dichloro-4-(((cyclohexylmethyl)(propyl)amino)methyl)phenyl)-2-(4-(methylsulfonyl)phenyl)acetamide ***(8c)***. Yield: 71%, white solid. ^{1}H NMR (400 MHz, $CDCl_3$) δ 7.89 (d, J = 8.3 Hz, 2H), 7.54 (s, 2H), 7.52 (d, J = 8.3 Hz, 2H), 3.80 (s, 2H), 3.72 (s, 2H), 3.06 (s, 3H), 2.38 (t, J = 7.2 Hz, 2H), 2.20 (d, J = 6.9 Hz, 2H), 1.74 (d, J = 12.0 Hz, 2H), 1.65–1.57 (m, 3H), 1.50–1.40 (m, 3H), 1.18–1.05 (m, 3H), 0.80 (t, J = 7.3 Hz, 3H), 0.69–0.59 (m, 2H). MS (ESI) *m/z*: 524.8[MH+].^{13}C NMR (101 MHz, $CDCl_3$) δ 167.89 (s), 140.58 (s), 139.57 (s), 137.52 (s), 137.22 (s), 130.41 (s), 127.92 (s), 119.21 (s), 61.10 (s), 56.24 (s), 53.83 (s), 44.56 (s), 44.07 (s), 35.80 (s), 31.84 (d, J = 10.5 Hz), 26.85 (s), 26.13 (s), 22.70 (s), 19.52 (s), 14.12 (s), 11.92 (s). HRMS (*m/z*): [MH$^+$] calcd for $C_{26}H_{34}Cl_2N_2O_3S$ 525.1740; found, 525.1740.

4.2.3. General procedure C for the synthesis of compounds (4a, 4h-4k)

Step 1. To a solution of nitrobenzene intermediates (1.0 eq), amine (3.0 eq) and anhydrous potassium carbonate (1.0 eq) in acetonitrile was added potassium iodide (0.1 eq). The mixture was heated up to 110 °C in microwave reactor for 30 min. Purification by column chromatography through silica gel afforded the desired intermediate **20.**

Step 2. To a solution of compound **20** (1.0 eq), 1-bromopropane (3.0 eq) and anhydrous potassium carbonate (1.0 eq) in acetonitrile was added potassium iodide (0.1 eq). The mixture was heated up to 110 °C in microwave reactor for 30 min. Purification by column chromatography through silica gel afforded the desired intermediate **21**.

Step 3. To a solution of **21** (1.0 eq) in methanol was added 10% Pd/C. The mixture was degassed and purged with hydrogen and stirred at room temperature for 1 h. The solution was filtered through celite and evaporated under reduced pressure to afford desired product **22** as white solid.

Step 4. To a solution of **22** (1.0 eq) in DCM was added *p*-alkylsulfone aryl acetic acid (1.2 eq), HATU (1.2 eq) and DIPEA (1.2 eq). The mixture was stirred at room temperature for 5 h. Purification by column chromatography through silica gel afforded desired compound (**4a, 4h-4k**)

*4.2.3.1. 2-(4-(ethylsulfonyl)phenyl)-N-(4-(2-(phenyl(propyl)amino)ethyl)phenyl)acetamide (****4k****).* Yield: 12%, white solid. ^{1}H NMR (400 MHz, $CDCl_3$) δ 7.78 (d, J = 8.0 Hz, 2H), 7.71 (d, J = 8.2 Hz, 2H), 7.47–7.39 (m, 4H), 7.34 (d, J = 7.3 Hz, 2H), 7.29 (t, J = 7.4 Hz, 2H), 7.21 (t, J = 7.1 Hz, 1H), 7.10–7.04 (m, 1H), 4.68 (d, J = 6.0 Hz, 2H), 3.54 (d, J = 12.7 Hz, 4H), 3.04 (q, J = 7.4 Hz, 2H), 2.38 (t, J = 7.1 Hz, 2H), 1.56–1.42 (m, 2H), 1.28 (dd, J = 15.3, 7.7 Hz, 2H), 1.21 (t, J = 7.5 Hz, 3H), 0.87–0.77 (m, 3H). MS (ESI) *m/z*: 465.2 [MH+]. ^{13}C NMR (151 MHz, MeOD) δ 170.79, 143.60, 138.47, 137.93, 131.38, 130.29, 129.50, 121.47, 54.41, 51.29, 49.65, 44.26, 33.87, 21.43, 11.65, 7.62. HRMS (*m/z*): [MH$^+$] calcd for $C_{27}H_{33}N_3O_3S$ 465.2206; found,

465.2201.

*4.2.3.2. 2-(4-(ethylsulfonyl)phenyl)-N-(4-(2-(phenylamino)ethyl) phenyl)acetamide **(4i)**.* Yield: 45%, white solid. ^{1}H NMR (400 MHz, $CDCl_3$) δ 7.84 (d, J = 8.2 Hz, 2H), 7.57 (s, 1H), 7.52 (d, J = 8.2 Hz, 2H), 7.41 (d, J = 8.3 Hz, 2H), 7.20–7.09 (m, 4H), 6.69 (t, J = 7.3 Hz, 1H), 6.59 (d, J = 7.9 Hz, 2H), 3.77 (s, 2H), 3.34 (t, J = 6.9 Hz, 2H), 3.10 (q, J = 7.4 Hz, 3H), 2.85 (t, J = 6.9 Hz, 2H), 1.24 (d, J = 4.2 Hz, 2H). MS (ESI) m/z: 423.2 [MH+]. ^{13}C NMR (151 MHz, $CDCl_3$) δ 167.84, 147.77, 141.19, 137.27, 135.99, 135.73, 130.24, 129.30, 128.60, 120.33, 117.65, 113.12, 50.64, 45.06, 44.05, 34.80, 7.39. HRMS (m/z): [MH^+] calcd for $C_{24}H_{27}N_2O_3S$ 423.1737; found, 423.1741.

*4.2.3.3. 2-(4-(ethylsulfonyl)phenyl)-N-(4-(phenethyl(propyl)amino) phenyl)acetamide **(4j)**.* Yield: 37%, white solid. ^{1}H NMR (400 MHz, $CDCl_3$) δ 7.86 (d, J = 8.2 Hz, 2H), 7.54 (d, J = 8.1 Hz, 2H), 7.31–7.26 (m, 4H), 7.23–7.19 (m, 1H), 7.17 (d, J = 7.5 Hz, 2H), 6.63 (d, J = 8.4 Hz, 2H), 3.76 (s, 2H), 3.48 (s, 2H), 3.20–3.06 (m, 4H), 2.81 (s, 2H), 1.59–1.46 (m, 2H), 1.30–1.26 (m, 3H), 0.87 (t, J = 7.4 Hz, 3H). MS (ESI) m/z: 465.2 [MH+]. ^{13}C NMR (151 MHz, $CDCl_3$) δ 167.44, 141.45, 137.36, 130.25, 128.73, 128.67, 128.56, 126.31, 122.32, 111.90, 50.66, 44.06, 11.39, 7.42. HRMS (m/z): [MH^+] calcd for $C_{27}H_{33}N_2O_3S$ 465.2206; found, 465.2199.

*4.2.3.4. N-(4-((benzylamino)methyl)phenyl)-2-(4-(ethylsulfonyl) phenyl)acetamide **(4a)**.* Yield: 66%, white solid. ^{1}H NMR (400 MHz, CD_3OD) δ 7.87 (d, J = 8.3 Hz, 2H), 7.71–7.65 (m, 1H), 7.62 (d, J = 8.1 Hz, 2H), 7.50–7.38 (m, 5H), 7.36–7.20 (m, 3H), 4.19 (d, J = 7.9 Hz, 2H), 3.82 (d, J = 8.6 Hz, 2H), 3.30–3.29 (m, 5H), 3.19 (q, J = 7.3 Hz, 2H). MS (ESI) m/z: 423.2 [MH+]. ^{13}C NMR (151 MHz, CD_3OD) δ 171.15, 143.33, 141.23, 138.58, 131.87, 131.43, 131.07, 130.78, 130.38, 129.51, 121.55, 52.02, 51.70, 51.28, 44.28, 7.62. HRMS (m/z): [MH^+] calcd for $C_{24}H_{27}N_2O_3S$ 423.1737; found, 423.1740.

*4.2.3.5. 2-(4-(ethylsulfonyl)phenyl)-N-(4-(phenethylamino)phenyl) acetamide **(4h)**.* Yield: 61%, white solid. ^{1}H NMR (400 MHz, $CDCl_3$) δ 7.85 (d, J = 8.2 Hz, 2H), 7.46–7.38 (m, 4H), 7.36 (s, 3H), 7.21 (d, J = 8.4 Hz, 2H), 6.58 (d, J = 8.3 Hz, 2H), 3.46 (t, J = 6.9 Hz, 2H), 3.12 (q, J = 7.5 Hz, 2H), 3.02 (t, J = 6.9 Hz, 2H), 1.92 (dd, J = 15.8, 7.6 Hz, 2H), 1.29 (t, J = 7.4 Hz, 3H). MS (ESI) m/z: 423.2 [MH+]. ^{13}C NMR (151 MHz, $CDCl_3$) δ 167.41, 145.44, 141.39, 139.15, 137.31, 130.24, 128.76, 128.64, 128.62, 126.46, 122.26, 115.57, 113.12, 50.64, 45.24, 44.00, 35.38, 7.41, 0.00.

4.3. RORγt dual FRET assay

The assay was performed in an assay buffer consisting of 50 mM NaF, 50 mM 3-(*N*-morpholino)propanesulfonic acid (pH = 7.4), 0.05 mM 3-[(3-cholamidopropyl) dimethylammonio]propanesulfonate, 0.1 mg/mL bovine serum albumin, and 10 mM dithiothreitol in 384-well plates. The total volume was 25 μL/well. The europium-labeled SRC1 solution was prepared by adding an appropriate amount of biotinylated SRC and europium labeled streptavidin into assay buffer, with final concentrations of 20 and 10 nM, respectively. The allophycocyanin (APC)-labeled-LBD solution was prepared by adding an appropriate amount of biotinylated RORγt-LBD and APC-labeled streptavidin at final concentrations of 20 and 10 nM, respectively. After 15 min of incubation at room temperature, a 20-fold excess of biotin was added and incubated for 10 min at room temperature to block the remain ning free streptavidin. Equal volumes of europium-labeled SRC and APC-labeled RORγt-LBD were dispensed into 384-well assay plates at 25 μL volume/well. The 384-well assay plates had 100 nL of test compound in DMSO predispensed into each well. The plates were incubated for 1 h at room temperature and then read on Envision in LANCE mode configured for europeum-APC labels.

4.4. RORγt GAL4 cell-based reporter gene assay

hRORγt LBD coding sequence was inserted into a pBIND expression vector (Promega, E1581) to express RORγt-GAL4 binding domain chimeric receptors. This expression vector and a reporter vector (pGL4.35 which carries a stably integrated GAL4 promoter driven luciferase reporter gene [luc2P/9XGAL4 UAS/Hygro]) were co-transfected into HEK293T host cells. Upon agonist binding to the corresponding RORγt-GAL4 chimeric receptor, the chimeric receptor binds to the GAL4 binding sites and stimulates the reporter gene. In the present of inverse agonist, agonist will bind competitively to the nuclear receptor and activate the reporter gene transcription. HEK293T cells were cultured in a culture medium composed of DMEM containing 5% charcoal-treated FBS at 37 °C under 5% CO_2 atmosphere, as ATCC recommended. Before assay, the cells were washed with PBS to remove phenol red and suspended in phenol red-free medium (phenol red-free DMEM containing 5% charcoaltreated FBS and Penicillin-Streptomycin (10,000 U/mL) to a proper concentration. 6×10^6 HEK293T cells were seeded into a 100 mm dish and incubated for 16 h. To a reagent mixture of *Trans*-IT reagent and Opti-MEM (Invitrogen) was added plasmid DNA (used as 0.5 mg/mL stocks), containing 5 μg RORγt plasmid and 5 μg pGL4.35 luciferase plasmid. The mixture was added to the cells in the 100 mm dish and incubated for 5–6 h. Test compounds were serially diluted in DMSO to 300 nM. Compounds (25 nL) were transferred into a 384-well plate (white opaque) using Echo550. Then seeded the cells at 15,000 cells/well into the 384-well plate using phenol red-free DMEM containing 5% charcoal-treated FBS and 0.25 μM ursolic acid. Cells were incubated for 16–20 h at 37 °C (white opaque) using Echo550 μL of Steady-Glo™ Luciferase Assay Reagent was added into each well of the 384-well plate. Shake the plate (avoiding light) for 5 min on a plate shaker. Record the luminescence value on Envision 2104 plate reader. Activation/Inhibition values of the compounds at 300 nM were determined by the average value of duplicated tests.

4.5. Mouse Th17 differentiation assay

$CD4^+$ T cells were purified from mouse splenocytes using a commercial $CD4^+$ T cell negative selection kit (Invitrogen). The 48-well plates were wrapped in the presence anti-CD3 (0.25 mg/mL, Bioxcel), and anti-CD28 (1 mg/mL, Bioxcel) at 0 °C overnight. $CD4^+$ T cells were skewed to Th17 cells by culturing cells in the presence of *anti*-IFNγ (10 μg/mL, Bioxcel), *anti*-IL-4 (10 μg/mL, Bioxcel), TGF-β (2 ng/mL, Peprotech) and IL-6 (20 ng/mL, Peprotech) for 4 days before analysis. Compounds or DMSO control were added to the culture on day 0 of Th17 differentiation at indicated concentrations. Percentage of IL-17 production from $CD4^+$ T cells were analyzed by intracellular staining followed by flow cytometry. Dose-response curves were plotted to determine half-maximal inhibitory concentrations (EC_{50}) for the compounds using the GraphPad Prism 5 (GraphPad Software, San Diego CA, USA).

4.6. Molecular docking studies

Molecular docking was carried out using Schrodinger 3.5 software package. The co-crystal structure of RORγt LBD (PDB: 4NIE, resolution of 2.01 Å) was selected and processed using the Protein Preparation Wizard including water deletion, addition of missing hydrogen atoms as well as adjustment of the tautomerization and protonation states of histidine. The compound 3D structures were subjected to energy minimization with force field (OPLS_2005) before submitting to the docking procedure. The docking grid was

centered according to the ligand position, and the bounding box was set to 11 Å. This docking was performed with Glide-docking using Extra Precision (GlideXP) algorithm. The final ranking from the docking was based on the docking score, which combines the Epik state penalty with the Glide Score. High-scoring complexes were inspected visually to select the most reasonable solution.

Declaration of competing interest

The authors declare that they have no known competing financial interests or personal relationships that could have appeared to influence the work reported in this paper.

Acknowledgements

This work was supported by National Natural Science Foundation of China(Grant Numbers: 81874287; 81973163; 82003577), Shanghai Bio-pharmaceutical Science and Technology Supporting Plan of China (Grant Number: 19431900100), National Science and Technology Major Project (Grant Number: 2018ZX09711002-003-014), Natural Science Foundation of Shanghai (Grant Number: 19ZR1436700) and China Postdoctoral Science Foundation (Grant Number: 2019M651383).

Appendix A. Supplementary data

Supplementary data to this article can be found online at https://doi.org/10.1016/j.ejmech.2021.113704.

References

[1] J. Couzin-Frankel, Breakthrough of the year 2013. Cancer immunotherapy, Science 342 (2013) 1432–1433.
[2] S.R. Jackson, J. Yuan, R.M. Teague, Targeting CD8+ T-cell tolerance for cancer immunotherapy, Immunotherapy 6 (2014) 833–852.
[3] D.M. Pardoll, The blockade of immune checkpoints in cancer immunotherapy, Nat. Rev. Canc. 12 (2012) 252–264.
[4] O. Boyman, M. Kovar, M.P. Rubinstein, C.D. Surh, J. Sprent, Selective stimulation of T cell subsets with antibody-cytokine immune complexes, Science 311 (2006) 1924–1927.
[5] L.A. Tesmer, S.K. Lundy, S. Sarkar, D.A. Fox, Th17 cells in human disease, Immunol. Rev. 223 (2008) 87–113.
[6] L.E. Harrington, R.D. Hatton, P.R. Mangan, H. Turner, T.L. Murphy, K.M. Murphy, C.T. Weaver, Interleukin 17-producing CD4+ effector T cells develop via a lineage distinct from the T helper type 1 and 2 lineages, Nat. Immunol. 6 (2005) 1123–1132.
[7] I. Kryczek, M. Banerjee, P. Cheng, L. Vatan, W. Szeliga, S. Wei, E. Huang, E. Finlayson, D. Simeone, T.H. Welling, A. Chang, G. Coukos, R. Liu, W. Zou, Phenotype, distribution, generation, and functional and clinical relevance of Th17 cells in the human tumor environments, Blood 114 (2009) 1141–1149.
[8] P. Muranski, A. Boni, P.A. Antony, L. Cassard, K.R. Irvine, A. Kaiser, C.M. Paulos, D.C. Palmer, C.E. Touloukian, K. Ptak, L. Gattinoni, C. Wrzesinski, C.S. Hinrichs, K.W. Kerstann, L. Feigenbaum, C.C. Chan, N.P. Restifo, Tumor-specific Th17-polarized cells eradicate large established melanoma, Blood 112 (2008) 362–373.
[9] Y. Miyahara, K. Odunsi, W. Chen, G. Peng, J. Matsuzaki, R.F. Wang, Generation and regulation of human CD4+ IL-17-producing T cells in ovarian cancer, Proc. Natl. Acad. Sci. U. S. A. 105 (2008) 15505–15510.
[10] I. Kryczek, S. Wei, L. Zou, S. Altuwaijri, W. Szeliga, J. Kolls, A. Chang, W. Zou, Cutting edge: Th17 and regulatory T cell dynamics and the regulation by IL-2 in the tumor microenvironment, J. Immunol. 178 (2007) 6730–6733.
[11] X. Su, J. Ye, E.C. Hsueh, Y. Zhang, D.F. Hoft, G. Peng, Tumor microenvironments direct the recruitment and expansion of human Th17 cells, J. Immunol. 184 (2010) 1630–1641.
[12] N. Martin-Orozco, P. Muranski, Y. Chung, X.O. Yang, T. Yamazaki, S. Lu, P. Hwu, N.P. Restifo, W.W. Overwijk, C. Dong, T helper 17 cells promote cytotoxic T cell activation in tumor immunity, Immunity 31 (2009) 787–798.
[13] Ivanov II, B.S. McKenzie, L. Zhou, C.E. Tadokoro, A. Lepelley, J.J. Lafaille, D.J. Cua, D.R. Littman, The orphan nuclear receptor RORgammat directs the differentiation program of proinflammatory IL-17+ T helper cells, Cell 126 (2006) 1121–1133.
[14] M. Robinson-Rechavi, H. Escriva Garcia, V. Laudet, The nuclear receptor superfamily, J. Cell Sci. 116 (2003) 585–586.
[15] Y. Wang, T. Yang, Q. Liu, Y. Ma, L. Yang, L. Zhou, Z. Xiang, Z. Cheng, S. Lu, L.A. Orband-Miller, W. Zhang, Q. Wu, K. Zhang, Y. Li, J.N. Xiang, J.D. Elliott, S. Leung, F. Ren, X. Lin, Discovery of N-(4-aryl-5-aryloxy-thiazol-2-yl)-amides as potent RORgammat inverse agonists, Bioorg. Med. Chem. 23 (2015) 5293–5302.
[16] M. Scheepstra, S. Leysen, G.C. van Almen, J.R. Miller, J. Piesvaux, V. Kutilek, H. van Eenennaam, H. Zhang, K. Barr, S. Nagpal, S.M. Soisson, M. Kornienko, K. Wiley, N. Elsen, S. Sharma, C.C. Correll, B.W. Trotter, M. van der Stelt, A. Oubrie, C. Ottmann, G. Parthasarathy, L. Brunsveld, Identification of an allosteric binding site for RORgammat inhibition, Nat. Commun. 6 (2015) 8833.
[17] T. Yang, Q. Liu, Y. Cheng, W. Cai, Y. Ma, L. Yang, Q. Wu, L.A. Orband-Miller, L. Zhou, Z. Xiang, M. Huxdorf, W. Zhang, J. Zhang, J.N. Xiang, S. Leung, Y. Qiu, Z. Zhong, J.D. Elliott, X. Lin, Y. Wang, Discovery of tertiary amine and indole derivatives as potent RORgammat inverse agonists, ACS Med. Chem. Lett. 5 (2014) 65–68.
[18] Y. Wang, W. Cai, T. Tang, Q. Liu, T. Yang, L. Yang, Y. Ma, G. Zhang, Y. Huang, X. Song, L.A. Orband-Miller, Q. Wu, L. Zhou, Z. Xiang, J.N. Xiang, S. Leung, L. Shao, X. Lin, M. Lobera, F. Ren, From RORgammat agonist to two types of RORgammat inverse agonists, ACS Med. Chem. Lett. 9 (2018) 120–124.
[19] R. Qiu, Y. Wang, Retinoic acid receptor-related orphan receptor gammat (RORgammat) agonists as potential small molecule therapeutics for cancer immunotherapy, J. Med. Chem. 61 (2018) 5794–5804.
[20] M.C. Yu, F. Yang, X.Y. Ding, N.N. Sun, Z.Y. Jiang, Y.F. Huang, Y.R. Yan, C. Zhu, Q. Xie, Z.F. Chen, S.Q. Guo, H.L. Jiang, K.X. Chen, C. Luo, X.M. Luo, S.J. Chen, Y.H. Wang, Crystallography-guided discovery of carbazole-based retinoic acid-related orphan receptor gamma-t (RORgammat) modulators: insights into different protein behaviors with “short” and “long” inverse agonists, Acta Pharmacol. Sin. (2020), https://doi.org/10.1038/s41401-020-00552-w.
[21] N. Sun, C. Yuan, X. Ma, Y. Wang, X. Gu, W. Fu, Molecular mechanism of action of RORgammat agonists and inverse agonists: insights from molecular dynamics simulation, Molecules (2018) 23.
[22] S. Xiao, N. Yosef, J. Yang, Y. Wang, L. Zhou, C. Zhu, C. Wu, E. Baloglu, D. Schmidt, R. Ramesh, M. Lobera, M.S. Sundrud, P.Y. Tsai, Z. Xiang, J. Wang, Y. Xu, X. Lin, K. Kretschmer, P.B. Rahl, R.A. Young, Z. Zhong, D.A. Hafler, A. Regev, S. Ghosh, A. Marson, V.K. Kuchroo, Small-molecule RORgammat antagonists inhibit T helper 17 cell transcriptional network by divergent mechanisms, Immunity 40 (2014) 477–489.
[23] B.P. Fauber, S. Magnuson, Modulators of the nuclear receptor retinoic acid receptor-related orphan receptor-gamma (RORgamma or RORc), J. Med. Chem. 57 (2014) 5871–5892.
[24] M.R. Chang, V. Dharmarajan, C. Doebelin, R.D. Garcia-Ordonez, S.J. Novick, D.S. Kuruvilla, T.M. Kamenecka, P.R. Griffin, Synthetic RORgammat agonists enhance protective immunity, ACS Chem. Biol. 11 (2016) 1012–1018.
[25] X. Hu, X. Liu, J. Moisan, Y. Wang, C.A. Lesch, C. Spooner, R.W. Morgan, E.M. Zawidzka, D. Mertz, D. Bousley, K. Majchrzak, I. Kryczek, C. Taylor, C. Van Huis, D. Skalitzky, A. Hurd, T.D. Aicher, P.L. Toogood, G.D. Glick, C.M. Paulos, W. Zou, L.L. Carter, Synthetic RORgamma agonists regulate multiple pathways to enhance antitumor immunity, OncoImmunology 5 (2016), e1254854.
[26] https://clinicaltrials.gov/ct2/show/NCT02929862?term=NCT02929862&draw=2&rank=1. https://clinicaltrials.gov/ct2/show/NCT03396497?term=NCT03396497&draw=2&rank=1.
[27] R.I. Olsson, Y. Xue, S. von Berg, A. Aagaard, J. McPheat, E.L. Hansson, J. Bernstrom, P. Hansson, J. Jirholt, H. Grindebacke, A. Leffler, R. Chen, Y. Xiong, H. Ge, T.G. Hansson, F. Narjes, Benzoxazepines achieve potent suppression of IL-17 release in human T-helper 17 (TH 17) cells through an induced-fit binding mode to the nuclear receptor RORgamma, ChemMedChem 11 (2016) 207–216.